HYPOTHESES FOR

SCRATCH BEHAVIOR OF

POLYMER SYSTEMS THAT RECOVER

Bernard Bujard, M.S.

Thesis Prepared for the Degree of

MASTER OF SCIENCE

UNIVERSITY OF NORTH TEXAS

May 2002

APPROVED:

Bruce Gnade, Chairman of the Department of Materials Science
Witold Brostow, Major Professor
Richard F. Reidy, Committee Member
Kevin Menard, Committee Member
Mohamed El Bouanani, Committee Member
Chester Neal Tate, Dean of the Robert B. Toulouse School of Graduate Studies

Bujard, Bernard, (Hypotheses for Scratch Behavior of Polymer Systems that Recover). Master of Science (Materials Science), May, 2002, 85 pages, 7 tables, 23 figures, references, 12 chapters.

Scratch recovery is a desirable property of many polymer systems. The reason why some materials have demonstrated excellent scratch recovery while others do not has been a mystery. Explaining the scratch resistance based upon the hardness of a material or its crosslink density is incorrect.

In this thesis, novel polymers were tested in an attempt to discover materials that show excellent scratch recovery – one of the most important parameters in determining the wear of a material. Several hypotheses were developed in an attempt to give an accurate picture of how the chemical structure of a polymer affects its scratch recovery. The results show that high scratch recovery is a complex phenomenon not solely dependent upon the presence of electronegative atoms such as fluorine.

ACKNOWLEDGMENTS

It is with great pleasure that I take this opportunity to thank my family for their patience and friends for their insight. I am forever indebted to my devoted supervisor, Prof. W. Brostow, for his professional and enthusiastic guidance throughout this work. To Julian Long the university thesis reader. Terry Glass from Dow Chemical Co. is acknowledged for his helpful providing of pure BLOX. I am also thankful to the University of North Texas at Denton for accepting me into their program and Notre Dame Seminary in New Orleans for their background in philosophy. And to God, the "Unmoved Mover", who motivated me and always tried to move me in the right direction.

TABLE OF CONTENTS

LIST OF TABLES

LIST OF FIGURES

PREFACE

"You do not write because you want to say something, you write because you have something to say."

F. Scott Fitzgerald

"The test of a first-rate intelligence is the ability to hold two opposed ideas in mind at the same time and still retain the ability to function."

F. Scott Fitzgerald

"An author ought to write for the youth of his own generation, the critics of the next, and the schoolmaster of ever afterwards."

F. Scott Fitzgerald

"Vitality shows in not only the ability to persist but the ability to start over."

F. Scott Fitzgerald

CHAPTER I

BACKGROUND FOR SCRATCH TESTING AND SOME CHARACTERISTICS OF SCRATCH RESISTANT MATERIALS

Scratch resistance is one of the most important service parameters. Nevertheless, scratch testing is an underappreciated area of Materials Science and Engineering (MSE). The scratch test was originally designed as a measurement of adhesion of thin hard films. Among the various techniques proposed for adhesion testing, the only one that led consistently to meaningful results and that could be used for quality control in large scale production is precisely the scratch test. The test was first proposed by Heavens in 1950 [1], and implemented in the 1960s by Benjamin and Weaver [2] who were also responsible for developing the first model for this behavior; however, their model failed to describe the behavior of hard coatings. The scratch test consists of deforming the surface by indentation under load of a moving rigid (e.g., diamond) tip. The applied load can be held constant, increased continuously, or increased stepwise. The smallest load at which the coating is damaged is called the critical load L_{cr} and is determined by optical or electron microscopy. In the case of very hard coatings the critical load is determined by acoustic emission. The critical load typically involves a graph representing the beginning of a continuously applied force. In 1985 Steinmann and Hintermann [3] used a scratch test method that relied upon an acoustic emission signal to determine the critical loads for TiC deposited by chemical vapor deposition upon various substrate materials. Their scratch test method reported data as an acoustic emission (AE) versus load L graph.

A fairly sophisticated scratch testing methodology was developed by Kody and Martin in 1996 and involved quantifying light scattered from solid polymer and polymer composite

surfaces due to surface deformation.[4] The technique is based on deforming the material in a controlled, reproducible manner. The machine uses a conical diamond stylus to induce scratches into a flat piece of a material mounted on a rotating stage. The results could then be used to compare the scratch resistance of materials with different compositions and different textures.

Historically, the scratch test is used for metals to determine hardness and for polymers to determine scratch recovery. Hardness is defined qualitatively as the characteristic ability of a material to resist penetration or abrasion by other bodies. However, any quantitative measure of this feature of material behavior depends on the technique used for its measurement; it is an extrinsic property of a material rather than a fundamental or intrinsic property such as density or thermal conductivity. [5]

The use of the ability of one material to scratch or abrade another as the basis of a scale of hardness perhaps preceded the use of indentation. They certainly ran in parallel for many years although it has been said that scratch tests have *not* been formalized to the extent as those depending on indentation. One of the earliest established hardness scales was that developed by Friedrich Mohs (1824). This scale is based on an array of ten minerals ranging from 1 (talc) to number 10 (diamond) – the latter being the same material as the indenter of most micro-scratch testers. Each member of the scale is capable of scratching all those numerically below it. There is, quite naturally, a strong correlation between the Mohs hardness of a material and that measured by indentation – see Figure I at the end of this chapter. The gradient of the Mohs scale is equivalent to an increase in indentation hardness by a factor of close to 1.6, with the exception of that from alumina to diamond. The evenness of this scale is a testimony to the careful experimental work of Mohs, who was well aware of the much larger step between the values of minerals 9 and 10. It is generally accepted that for one material to scratch another, the indenter

or scratching particle must be at least 20 % harder than the damaged surface. Actually, this factor depends rather on the shape of the scratching particle, varying between only just over unity for a close to spherical particle to about 1.6 for a much more angular indenter with a non-diamond tip. [5]

Any form of scratch hardness test is a form of controlled abrasive wear, and, thus, it seems reasonable to use the test as a means of ranking materials according to their relative resistance to wear in service. This must be done with caution since the geometry of the scratch hardness indenter is likely to be very different (usually very much more severe) from the comparatively rough surfaces that make up the topography of surfaces that appear to be smooth. Neither is it easy to relate the measured scratch hardness to other, perhaps more fundamental material properties such as elastic modulus or yield stress because there is not, at least at the present time, a complete deterministic model of the scratching process in the literature. In practice, scratch testing was most often used as a quality control technique enabling the performance of one surface to be qualitatively and, to some extent, quantitatively compared to another which is known to be satisfactory in use. This form of test is especially popular when dealing with surfaces that have been engineered by thermal, chemical or coating treatments in order to give them enhanced hardness or wear resistance. [5]

Around the turn of the century, the Swedish metallurgist Brinell was responsible for developing the technique of pressing a hard sphere into the test surface (an indentation test) to assess a material's strength or resistance to deformation and the test is still widely used. The Brinell hardness H_B is simply defined as the load per unit curved area of the indenter:

$$H_B = 2P / \pi D^2 \{1 - (1 - (d/D)^2)^{1/2}\} \qquad (1)$$

Where P is the applied load, D is the diameter of the sphere and the measured diameter of the resulting permanent depression is d (which we call the residual depth). [5] Since the sample is not moving, the applied load is static in comparison to a scratch test that has a constant or progressively increasing applied load. For this reason, equation (1) should not be used to attempt to convert scratch test data into a number representing Brinell Hardness.

A significant disadvantage of this test is the fact that the hardness depends on the ratio of d/D; this means that changing either the diameter of the test ball or the load P can lead to different numerical values of the hardness for a given surface. This particular problem is overcome in the Rockwell hardness test that uses a spherically tipped conical indenter with the included angle of 120˚. There are also Vickers and Knoop tests which both use pyramidal indenters. The Vickers indenter, introduced in the late 1920's has the angle of 136˚ between opposing faces – this was chosen to be 'equivalent' to the Brinell test in which the ratio d/D was equal to 0.375. The Knoop indenter is such that it forms an elongated rhombic indentation in which the longer dimension is seven times the smaller dimension. The Knoop test is particularly useful for studying the indentation resistance of relatively brittle materials and investigating the effect of crystal structure on hardness. [5]

At about the time when the scratch hardness tests were still competing with the indentation tests for commercial acceptance a number of possible geometries were suggested for the scratch test. For example, in the Birnbaum test the corner of a cube is dragged across the test surface with the leading edge diagonal inclined at an angle of 35˚ to the direction of scratching. However, for general engineering use indentation hardness triumphed over scratch hardness - the scientific community tending to work mainly with Vickers or Knoops figures while commercial and industrial materials are often quoted in Brinell or Rockwell values. [5]

The Vickers hardness H_V of a surface is defined as the applied load P divided by the surface area of the sloping sides of the pyramidal indentation. [5] Since it is usually the length w of the diagonals of the impression that are measured, it follows from the geometry of the indenter that

$$H_V = (\text{load P} / \text{diagonal}^2) \bullet 2\sin 68^\circ \qquad (2)$$

$$= P / w^2 \bullet 1.854$$

Now consider what happens if a static Vickers hardness test is turned into a scratch test by maintaining the normal load at P but moving the indenter, say along a direction of one of the diagonals of the indentation. At first the indenter will sink further into the surface as a result of the loss of the load carrying capacity of the rear two faces. As the movement proceeds, the indenter will tend to push a wedge of deforming material ahead of it. A steady state will be reached in which both the normal force P, the tangential force F and the extent of the plastic deformation (which is usually measured by the width of the resulting groove left in the surface) become constant. In principle it actually makes no difference whether the indenter traverses the sample edge forward or face forward although the edge forward is the most common. Comparison between hardness values made with pyramidal indenters and those made with a conical or Rockwell indenter can be made if an equivalent pyramid angle is chosen which would have generated the same displaced volume of material. [5]

In practice the scratch hardness H_S is rarely equal to the static indentation hardness H_C; this is true for even ductile metals. If one were to use an indenter to measure scratch hardness consistently, then the optimum cone or pyramid angle must lie in the range of 120° to 160°. Indenters with smaller angles, and so larger effective attack angles, are more likely to produce significant volumes of debris by micro-machining. Elastic deformation in the back of the scratch can be significant in scratch tests that use indenters of large angles. [5]

Most earlier tribological results pertain to metals. With brittle solids, the high "hydrostatic pressures" developed around the deformed region may be sufficient to inhibit brittle fracture; under these conditions both indentation and scratch hardness are measures of plastic rather than brittle properties of the solid. When fracture does occur, it may often be driven by the stresses associated with the mismatch between conditions in the plastically deforming zone and the surrounding material within which conditions are elastic. Cracks may often propagate as a material is unloaded, that is effectively behind the indenter in a scratch test. [5]

S.J. Bull in 1999 asked the question, "Can scratch testing be used as a model for the abrasive wear of hard coatings?" – also the title for his paper. [6] He discussed the relationship between the wear rate and hardness and scratch testing parameters for TiN coatings on 304 stainless steel deposited by three deposition technologies. He concluded that the correlation between wear resistance and hardness is poor, but the correlation with interfacial shear strength determined in the scratch test is only marginally better. In general, as the interfacial shear strength increases the wear rate of the system decreases. However, the balance between the deformation mechanisms which control this shear strength (fracture, plasticity, and coating detachment) changes as the coating thickness (and substrate hardness) increases and choosing an appropriate scratch test load to mimic this is not possible. He writes, "The scratch test in its current form can thus be used to generate the same damages as are observed in abrasive wear but cannot simply be used to make a quantitative prediction of wear rate." [6]

Bull also notes that the effect of grain size in controlling hardness often manifests itself in the variation of hardness with coating thickness. As the coating thickness increases, and its grain size also increases, the hardness decreases. He also concluded that the hardness behavior of the system is dominated by the substrate. The presence of unreacted titanium in these films has the

advantage of reducing stress but can compromise the properties of the coatings in other ways. For all deposition technologies, the critical load for coating detachment increases with coating thickness. The arc evaporated TiN films have a lower critical load than comparable sputtered films. This is due to the presence of unreacted titanium in the film that dramatically increases the friction measured during the scratch test. The critical load for coating detachment is also reduced for the coatings deposited on the softer mild steel substrate. [6]

There is not a strong correlation in wear rate with coating thickness though there is a tendency for the wear rate to decrease with increasing coating thickness for all but the thinnest coatings. In general, hardness is *not* a good guide to the abrasive wear resistance of many coatings. The scratch test can give information about plastic deformation and fracture and coating detachment but the critical load for coating detachment does not contain information about the wear of a material. [6]

Ahila, Reynders and Grabke (1996) investigated the repassivation of Cr-Mn and Cr-Ni steels at room temperature in a sodium sulfate + sodium chloride solution mixture in the presence of electronegative nitrogen. The Cr-Mn steels with 0.0075, 0.6 and 0.9 % nitrogen were scratch tested at different passive potentials. The Cr-Mn steel with only 0.0075 % nitrogen was found to undergo grain boundary corrosion. The grain boundary attack occurred along both the scratched and the unscratched area with no preference for one over the other. The higher content of nitrogen in 0.9 % compared to 0.6 % Cr-Mn steels did not improve repassivation – the repassivation was approximately the same. In these two alloys with high nitrogen content the scratches had not acted as the sites for pitting. [7]

Cr-Ni steels also exhibited repassivation in the presence of 0.7 weight % electronegative nitrogen. The effect of nitrogen was observed in these steels also, though not to the same extent

as in Cr-Mn steels. It can be stated that nitrogen improves the repassivation tendency of all steels investigated. Repassivation should be regarded as a significant mechanism for scratch healing and recovery in metals. When there is no nitrogen in the steel, pitting has occurred in both places – along the scratch or on the unscratched area. The major role of nitrogen appears to be in favoring the repassivation rather than in preventing the pit formation. Thus, pit formation was not prevented totally in nitrogen alloyed steels (as pits were seen on unscratched areas), but the pit growth was hindered by the fast repassivation kinetics of high nitrogen steels. It should be noted that the effects of electronegative chloride were almost the exact opposite: (1) a reduction of the repassivation rate, (2) an increase of repassivation time, and (3) the occurrence of metastable or stable pitting. The repassivation rates in solutions free of chloride were all quite high. [7]

There are different models to explain the effect of nitrogen on the localized corrosion resistance of alloys. They include (1) consumption of acid in pit nuclei by nitrogen dissolution and ammonium ion formation, (2) enrichment of nitrogen on the passivated surfaces at the film/metal interface which may lead to desorption of the aggressive anions (Cl^-) upon breakthrough of the passive layer, and (3) enrichment of nitrogen on the active surfaces thus inhibiting pit initiation. [7] Chapters VIII and XI discuss the effects of nitrogen in increasing scratch resistance and recovery in polymer systems.

A friction test is basically different from a micro-scratch test. The standard test method for determining the static and kinetic coefficients of friction of plastic film and sheeting are outlined in ASTM Standard D 1894 – 90. [8] There are three basic laws characterizing quantitatively the frictional resistance: [9]

1. The total frictional force F_f tangential to a surface is directly proportional to the force F normal to the surface:

$$F_f = \beta_f F \qquad (3)$$

Here the proportionality factor β_f is called the coefficient of friction, and from now on simply referred to as friction.

2. The frictional force is independent of the apparent area of contact. Therefore, large and small objects of the same material have the same friction.

3. The force necessary to start the motion is called the static friction. The force necessary to maintain a steady relative motion is called the kinetic friction and it is nearly independent of the relative velocity of the two surfaces.

While the friction test has an ASTM standard, the scratch test has no ASTM standard, hence its use is left to the discretion of the user who designs an experiment based on previous knowledge of the material and the particular scratch tester. All parameters that can be changed must be recorded in order for reproducibility. In addition, Spuzic, Strafford, Subramanian and Green [10] report that all scratches produced on surfaces under tension exhibited a greater scratch depth when compared with scratches made on surfaces exposed to compression – increases in scratch depth of more than 15 % were observed! For this reason, it is recommended that samples are mounted to avoid compressional or tensional forces. Also, scratches made on surfaces with a cyclic stressing history are deeper than scratches made on surfaces without a cyclic stressing history. These are all important parameters that must be recorded when making comparisons between materials. [10]

The principal approach in a study by Spuzic, Strafford, Subramanian and Green was to create testing conditions and measure the relevant responses that conform to specific real situations without developing a special device for such a purpose. "The wear literature contains literally hundreds of 'one-of-a-kind' testing machines, and it would appear that their number far exceeds the (actual) number of 'standard' wear testing devices." [10] There is therefore an advantage in the more effective use of an existing apparatus (such as a micro-scratch tester by CSM) "with minimum adjustments, to broaden existing data bases and enable utilization and application of well-known analogies and approximation principles." [10]

Some users claim that there exists a set of generally accepted parameters and testing procedures. Bennett and Matthews explain that, "In all areas of testing, especially in the field of tribology, standard conditions must be defined and applied if laboratories are to produce comparable results." The standard conditions for scratch testing used by Bennett and Matthews are: scratch speed 10 mm/min; loading rate 100 or 10 N/min; indenter tip radius 200 microns; Temperature 20 $\pm$ 2˚C; Humidity 50 $\pm$ 5 % relative humidity. [11]

Although the static and dynamic coefficients can be determined with a special friction table mounted to a scratch tester, a scratch test and a friction test are unique. There are three basic laws characterizing quantitatively the scratch recovery using our Micro-Scratch Tester:

1. Whereas the applied force for a friction test is *tangential* to the surface, the applied load for a scratch test is *normal* to the surface. The Micro-Tester can be used to test the friction β_f once the friction table is installed by using the following equation:

$$\beta_f = \text{tangential force / normal applied force} \qquad (4)$$

2. Whereas the frictional force is independent of the apparent area of contact (as determined by the dimensions of the sample), the amount of scratch recovery is directly related to the amount of initial penetration depth made by the indenter, and this is directly related to the apparent area of contact made by the indenter.
3. Both the friction test and the scratch test demonstrate a characteristic initial required force to start the motion. Whereas in the friction test this is referred to as the static friction, in the scratch test this initial force is a little more complicated. For our scratch test method the minimum applied load must be at least 0.01 N. If the sample to be tested is a metal, then the initial applied force to just cause a noticeable scratch as viewed under the optical microscope or by acoustic emission is referred to as the critical load. If the sample is a polymer, the action of the indenter applying a very light load and just getting started causes a "jumpy" motion between the two surfaces which often gives a rough-looking graph at the very beginning of the plot. Typically, the beginning of the scratch for a polymer with a recoverable surface will largely heal – determining the critical load is impractical except in the case of non-recoverable surfaces.

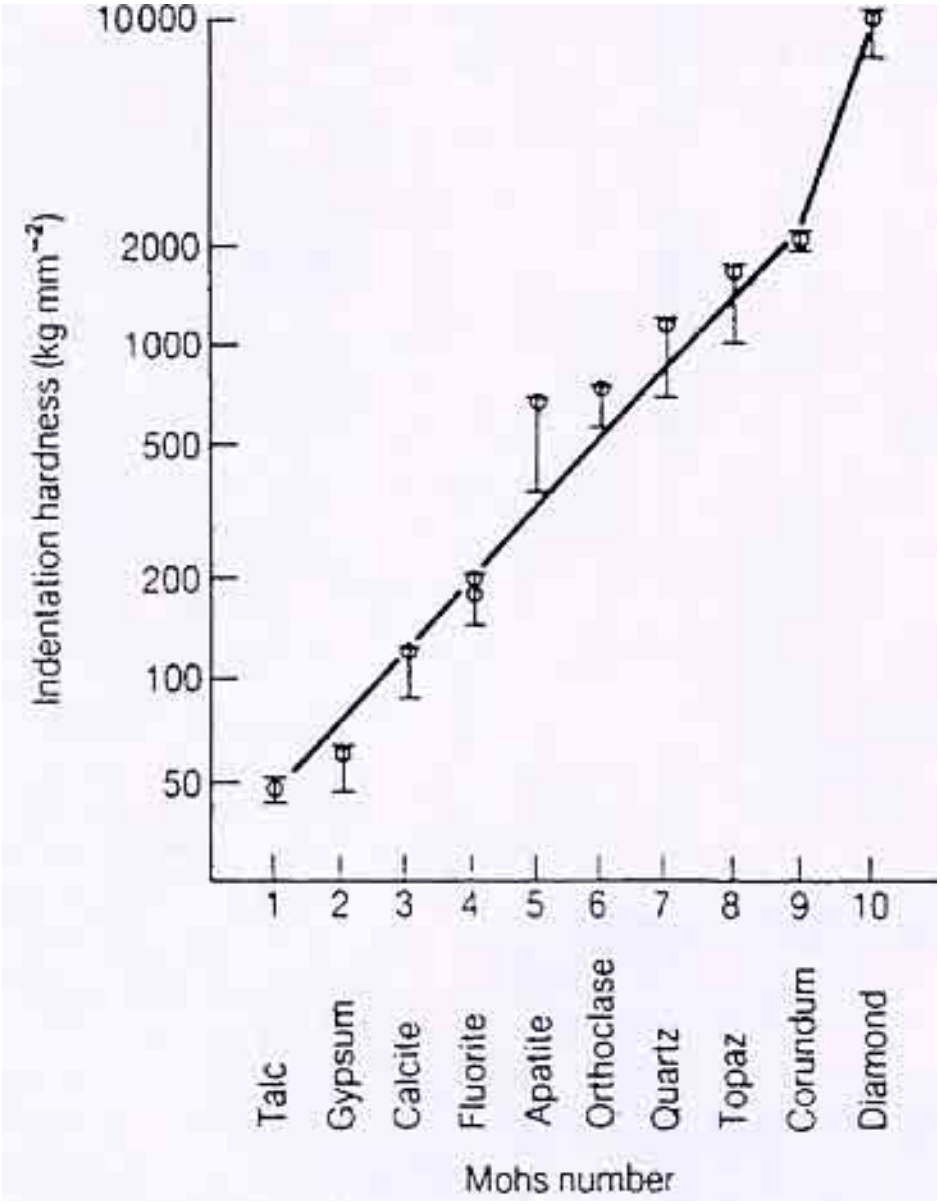

Figure I. Mohs scale of hardness when plotted against a Vickers scale of indentation hardness gives the slope of the line indicating a hardness factor of 1.6 between adjacent minerals on the scale. The slope of the line from corundum (a form of alumina) to diamond is an exception. It is generally accepted that for one material to scratch another, the indenter or scratching material must be at least 20 % harder than the damaged surface.[5]

CHAPTER II

PROCEDURES

II.1. Previous micro-scratch and nano-scratch test procedures

Benayoun, Hantzpergue and Bouteville performed micro-scratches using a system equipped with an optical microscope, an acoustic emission sensor and a friction force sensor. [12] Critical loads were determined to evaluate the adhesion of TiN to the substrate. They observed the damage along the scratch track and noted different types of damage for increasing applied loads. For weak loads, very narrow parallel grooves were first formed in the track center. As the load increased, induced cracks were formed behind the tip. These cracks were regular, perpendicular and parallel to the scratch if the scratch direction was parallel to the cleavage planes of the silicon monocrystal. Scratches carried out in random directions have shown that the first cracks formed were following the silicon cleavage planes independently of the scratch direction. The beginning of TiN film detachment was located shortly behind, or on, the transversal cracks within the scratches. No large film area was removed as is generally shown in scratch tests for polymeric materials, but small TiN chips were observed. For slightly higher loads, a network of "behind cracks" was superimposed on the network of cracks produced ahead of the tip. [12]

Bennett and Matthews [11] note the obvious fact that in all areas of testing, especially in the field of tribology, standard conditions must be defined and applied if laboratories are to produce comparable results. They suggest that the scratch test, like any other tribological test such as friction testing, must have the operating temperature and humidity defined. At present, most scratch testing equipment does not have environmentally controlled test conditions. [11] This

author agrees that the operating temperature must be specified if the scratches are not performed at room temperature (about 24°C).

Consiglio, Randall, Bellaton and von Stebut [13] use a nano-scratch tester (NST) that exploits the normal force range from 10 μN to 1 N. In comparison, our micro-scratch tester is capable of testing the range, 0.01 N to 30 N, but typically our procedure calls for a range of 0.03 N to 15 N. They test primarily for what they call "mar". They explain that the difference between mar and scratch resistance is that mar, for example, is related only to the relatively fine surface scratches which spoil the appearance of an automotive coating. Because of the very small tip radius (10 μm), the NST is suited to simulating such scratch damage in a controlled way, for example, damage caused in service due to car washing, polishing, grit impact, or other very fine scratches as a result of environmental conditions. [13]

Hedenqvist and Hogmark [14] claim that more than 20 methods for adhesion assessment are proposed in the literature, but the only methods that are applicable to hard, well-adherent coatings are the laser photoacoustic shockwave test, indentation and the scratch adhesion test. The scratch test is by far the most widely used and "the most straightforward method for monitoring the scratch testing is optical microscopy". [14] They also note that a procedure that calls for an occasional inspection or changing of the indenter diamond tip is necessary. "As the diamond indenter wears, the stress field created by it alters. This will, in turn, naturally affect the scratch test results. In order to minimize diamond tip wear, the diamonds should be oriented along the (100) direction. Wear or occasional brittle fracture, however, still occur, and it is recommended that the diamond tip is inspected at regular intervals. " [14]

The author of this thesis agrees with Hedenqvist and Hogmark that we will experience an increasing use of the scratch test to obtain a variety of information on coatings or

coating/substrate composites and that there are many alternative uses for the scratch tester equipment – "the creativity of the user is the only limiting factor!" [14] With this idea in mind, it would seem difficult to write an ASTM standard procedure regarding scratch testing that encompasses the full range of materials and alternative uses for scratch tests.

Jardret, Zahouani, Loubet and Mathia [15] state that whatever scratch testing procedure one uses, the contact area, the scratch width, the residual scratch width and the tip geometry must be accurately known. "In scratch testing the key to accurate analysis is to appropriately estimate the contact area during the experiment. The groove width, so determined, will then be used to calculate the contact area using the tip geometry. In this procedure, we assume that the deformation recovery remains in a vertical plan parallel to the scratch direction. The residual scratch width is very important in estimating the actual contact area in conjunction with the indenter geometry....". [15] Our procedure and most present scratch testing procedures are slightly different. The initial scratch depth and the residual (recovery) depth are regarded as more important than the scratch width and residual scratch width. These factors along with the tip geometry and radius determine the percent of recovery.

A procedure by Malzbender and de With [16] specified using spherical indenters with a radius of 20, 150 and 500 microns on organic-inorganic coatings. They determined that the *critical load* for the initiation of surface cracks is probably not significantly influenced by the underlying substrate. However, the path of the crack in the perpendicular direction will be significantly influenced by changes in the stress intensity due to the underlying substrate. Of the indenters investigated the critical load is only slightly larger for the softer substrate using the 150 micron sphere. [16]

Malzbender and de With [16] determined that variations in the indenter radius are significant - all critical loads increase with increasing indenter radius. This seems logical since the force per unit area decreases as the radius of the tip increases – a larger critical load will be needed to obtain the same failure. Therefore, one must always report the indenter radius when giving the results from a scratch test. The degree of uncertainty in the measurements is also proportional to the indenter radius. The results obtained using a large spherical indenter show a larger uncertainty in indentation depth and applied load than the results obtained using a small sphere. They believe that this might be related to the roughness of the sphere. Also, the scratch hardness H_s decreases with increasing indenter radius R. [16]

The effects of varying the scratch speed were investigated by Malzbender and de With. An increase of only the scratching speed increases the number of cracks per unit load in a brittle material but not per unit length. Thus, the number of cracks appears to depend primarily on the contact area. This relationship has been used in a separate work to estimate the crack density. For the 150 micron sphere increasing the scratch speed from 2 to 50 microns/second has no effect on the penetration depth or the accuracy of the measured applied load. [16]

Randall, Favaro and Frankel [17] also support the findings by Malzbender and de With in their studies of polymeric paint coatings on aluminum substrates. As a general rule, the measured critical load (for a metal) is seen to increase quite dramatically as the indenter radius is increased. In some cases (e.g., W), the critical load increases by an order of magnitude between 20-μm and a 200-μm indenter radius. This clearly demonstrates the importance of indenter choice when making comparative measurements. However, the elastic recovery is higher when large radius indenters are used because of the "hydrostatic nature of deformation". [17]

Randall, Favaro and Frankel found that the critical load is seen to decrease as the scratching speed is increased. The overall critical load values increase with increasing loading rate; however, they comment that other studies have shown the loading rate and scratching speed have no prominent effect on the critical load. It can be summarized that the dependence of critical load on loading rate and scratching speed is highly influenced by the particular *coating-substrate material pair* measured. Randall, Favaro and Frankel suggest that when quoting practical values of adhesion, it is imperative that all parameters which can influence the results be mentioned in the procedure if truer comparisons are to be made. [17]

II.2. The LAPOM micro-scratch test procedure

Brostow, Cassidy, Hagg, Jaklewicz and Montemartini at LAPOM (Laboratory of Advanced Polymers and Optimized Materials) in the University of North Texas have shown that: (1) samples with high fluoropolymer concentrations exhibit elevated elastic modulae and are highly ductile, (2) fluoropolymer systems cured at 70˚C can have more compact structures due to faster crosslinking than at room temperature and (3) an increase in toughness was observed for the fluoropolymer systems under investigation. [18] However, changes in ductility, crosslinking or the toughness of a material will not alone tell us if a material will resist scratching.

A scratch test procedure was developed for our polymers using an already existing instrument - a Swiss micro-scratch tester (MST) from CSM Instruments (formerly CSEM) utilizing the CSM Scratch Software Version 2.3. After the data was gathered the files were converted into an Excel file and re-graphed for comparison purposes using Microsoft Excel 97.

The principle is the same whether the scratch test is performed in either a constant or progressively increasing applied load. A Rockwell diamond tip with a point radius of 200 μm,

the indenter, is applied normal to the surface with an applied force ranging from 0.01 N to 30 N. This load can be held constant, however, the progressively increasing mode is usually preferred in order to observe the effects of a full range of applied forces in one scratch. [19]

The indenter passes three times over the surface for each scratch test. An initial pass or pre-scan is performed at the very light load of 0.03 N to determine the roughness of the surface before the actual scratch is administered. The second pass consists of the actual scratch. Typically, the initial scratch is made with a progressive load of 0.03 N to 15 N at the scratch speed of 5.259 mm/min and this determines the initial penetration depth at these applied forces. The scratch length is 5 mm. The final pass of the indenter, the post-scan, determines the amount of depth recovery after the initial penetration of the indenter. A very low force of 0.03 N is again applied to the surface during the post-scan to determine the amount of scratch healing. [19] Typically, this measurement is taken within 5 minutes of the initial scratch. In the present work a minimum of 10 scratches are performed for each sample, except where otherwise noted, and the averages are reported. All scratches have been made at room temperature – about 24˚C.

The scratches are observed under the optical microscope in order to verify that a scratch exists and to achieve correspondence between any unusual points in the graph to what actually appears under the microscope. The optical microscope is a morphological tool that gives contrasts based on differences in refractive indexes. Most scratches show a characteristic "teardrop-shape". The scratch, as viewed through the optical microscope, begins at a point and gradually widens and deepens as the applied force steadily increases from 0.03 N to 15 N. With most metals like stainless steel the scratch will appear the same under the optical microscope immediately after the scratch and several minutes later. However, with viscoelastic materials such as our polymers the appearance of the scratch may change with time. Typically all polymers

demonstrate some degree of scratch recovery while fluoropolymers, polymers engineered to have the optimum ratio of electronegative groups, have a high amount of scratch recovery.

The penetration depth of the scratch was plotted versus the applied force in Newtons. The same plot was performed for the residual depth. The accuracy of the depth determination is $\pm$ 7.5 nm, far more than sufficient for our purposes since we report in this work effects of the order of microns or hundreds of microns. This margin of error is less than the typical line widths used to plot the graphs. The residual or recovery depths are compared to the penetration depths. These are plotted as % recovery versus the applied force in Newtons using the following formula expressed in its general form:

$$\% \text{ recovery} = (1 - \text{Recovery Depth}/\text{Penetration Depth}) \bullet 100\ \% \qquad (5)$$

II.3. How useful is DOE (Design of Experiment) in developing a procedure for optimum scratch recovery materials?

The Taguchi method can reduce the number of experiments by avoiding an unnecessary repetition of factors in an experimental design. But can the Taguchi method be used as a successful tool in sample preparation? Yes, if each *method* of sample preparation is regarded as an experiment in itself, then the Taguchi method should be successful in facilitating a researcher in sample preparation. [20] The Taguchi method uses partial factorials, and we chose it since it is a very simple and easy experimental design; however, it has its limitations, and there are presently other preferred experimental designs.

Ordinary epoxies will decompose instead of melting when heated; however, a *thermoplastic epoxy* has characteristics of both an ordinary commercial epoxy and a thermoplastic. An *ordinary* commercial epoxy consists of two parts: (1) a liquid containing many long chain macromolecules and (2) a liquid that serves as a curing agent to form extensive crosslinking of

these macromolecules. BLOX (received courtesy of Dow Chemical Co.) is an experimental thermoplastic epoxy made from two separate components that are mixed together to form crosslinks while hardening. However, the difference between this epoxy and an ordinary epoxy is that BLOX can be melted like any other thermoplastic material – see SEM image in Figure II. The sample preparation in this case is more complex since now the samples can be prepared with or without solvents and with our without using the oven. The Taguchi method was used to determine the optimum number of samples to prepare based upon the possible combinations of these factors. Table I at the end of this chapter summarizes the conditions. [20]

The solvent for BLOX was tetrahydrofuran (THF). However, the sample could also be prepared without solvent if it were placed in an oven above the glass transition temperature at exactly 155°C – the "High" temperature in Level I. Both Level I and Level II represent two well-defined routes for sample preparation – therefore L = 2. "Short time" in this case represents 4 hours while long time represents 1 week. Given the Taguchi formula for

$$\text{Number of Experiments (NOE)} = F (L - 1) + 1 \qquad (6)$$

then L=2, F=3 since there are 3 significant factors (F), then 3 (2-1) + 1 gives 4. The Taguchi method suggests that we must prepare a minimum of 4 samples or 4 combinations of the factors for A, B and C – temperature, solvent, and curing time. An L4 array appears in Table II. [20]

The L4 array suggests that 4 combinations of sample preparation should be attempted. A sample prepared at 155°C, using no solvent and left in the oven for 4 hours – combination (111). A second sample prepared at 155°C, with solvent and left in the oven for one week – combination (122). A third sample prepared at room temperature, using no solvent, and left at room temperature for one week – combination (212). And the Taguchi method suggests that the fourth and last sample should be prepared at room temperature, with solvent, and allowed to cure

for only 4 hours – combination (221). Obviously, this experiment involves only 1 repetition. The same 4 combinations of factors could be repeated several times if necessary but the Taguchi method suggests that for only 1 repetition 4 samples must be prepared involving the 4 possible combinations of factors. [20]

A bit of common sense should also be used when applying the Taguchi method. Run 2 gives a combination of (122) or suggests that the sample should be prepared at 155°C, with solvent and left in the oven for one week. Obviously, the Taguchi method does not take into account the rate of evaporation of the solvent, that the solvent may be flammable, or that the polymer may degrade after being left at 155°C for one week. One must be careful when using the Taguchi method in sample preparation if there are known hazards. Basically, the Taguchi method ensures that all possible combinations of sample preparation procedures are considered based upon the variables available. [20]

We have established (see Chapter VI) that fluoropolymer blends demonstrate higher scratch recovery when blended with an epoxy matrix in small concentrations; however, the material blended with the BLOX matrix is not a fluoropolymer but a polymer we have called LB-22. (BLOX + LB-22 gives an average scratch recovery of about 88 %, discussed in Chapter XI, without the presence of potential environmentally unfriendly fluorine atoms.) This material compares very competitively with the scratch recovery results of a fluoropolymer + epoxy blend. Therefore, since we make samples at low concentrations of 0 %, 5 %, 10 %, 15 %, and 20 % LB-22, the Taguchi method suggests that we should make a minimum of 4 samples using different combinations of the factors at each concentration or a total of 20 samples – assuming only one repetition per concentration. The recommended minimum number of scratches to perform on a sample, 10, is very highly dependent upon the type of material and whether or not

phase separations occur and is not determined by the Taguchi method; poorer surfaces may require a higher minimum.

The Taguchi method suggestion for preparing a minimum of 4 methods of sample preparation involving the combinations of factors sounds very reasonable in the case of BLOX since it is well known for having a tendency to produce some bubbles in the sample – see SEM image in Figure III. BLOX is a very effective vapor barrier. This SEM image is unusual since the bubbles appear to form first from primary bubbles that enlarge to produce numerous secondary bubbles. Most of these secondary bubbles appear with dark spots or holes that may be occurring during sample preparation as these "thin-skinned" secondary bubbles under pressure apparently burst. These bubbles often make the sample surface too rough for scratch testing and are much more numerous whenever an evaporative solvent is used. When these bubbles are located at the surface of the sample they are often an indication of trapped solvent or water vapor; however, Chapter IX offers an alternative explanation for the suppressed evaporation of THF in BLOX. The combination of (111) or sample preparation at 155°C, no solvent and keeping in the oven for only 4 hours was eventually determined to be the best method of sample preparation under these conditions for BLOX + LB-22.

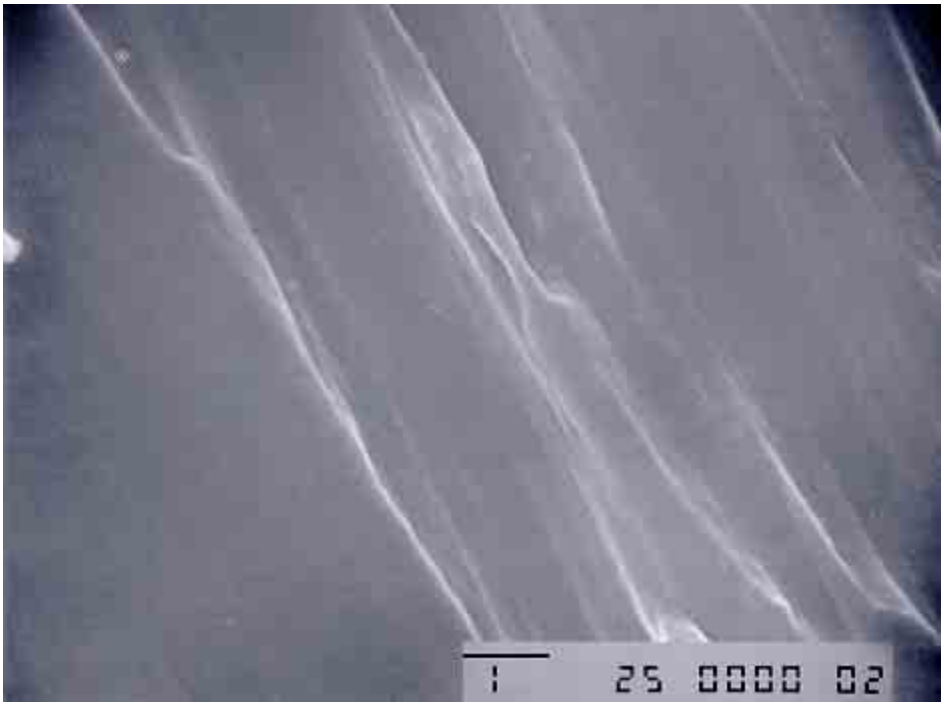

Figure II. An SEM image of a pure BLOX pellet. The striations upon the surface are parallel to the longitudinal axis of extrusion. As the polymer was extruded it was diced into pellets.

TABLE I - Factor Listing for L4

FACTOR	Level I	Level II
A. Temperature	(1) High	(2) Room Temperature
B. Solvent	(1) No Solvent	(2) Solvent
C. Curing Time	(1) Short Time	(2) Long Time

TABLE II - The L4 Array

RUN	A. Temperature	B. Solvent	C. Curing Time
1	1	1	1
2	1	2	2
3	2	1	2
4	2	2	1

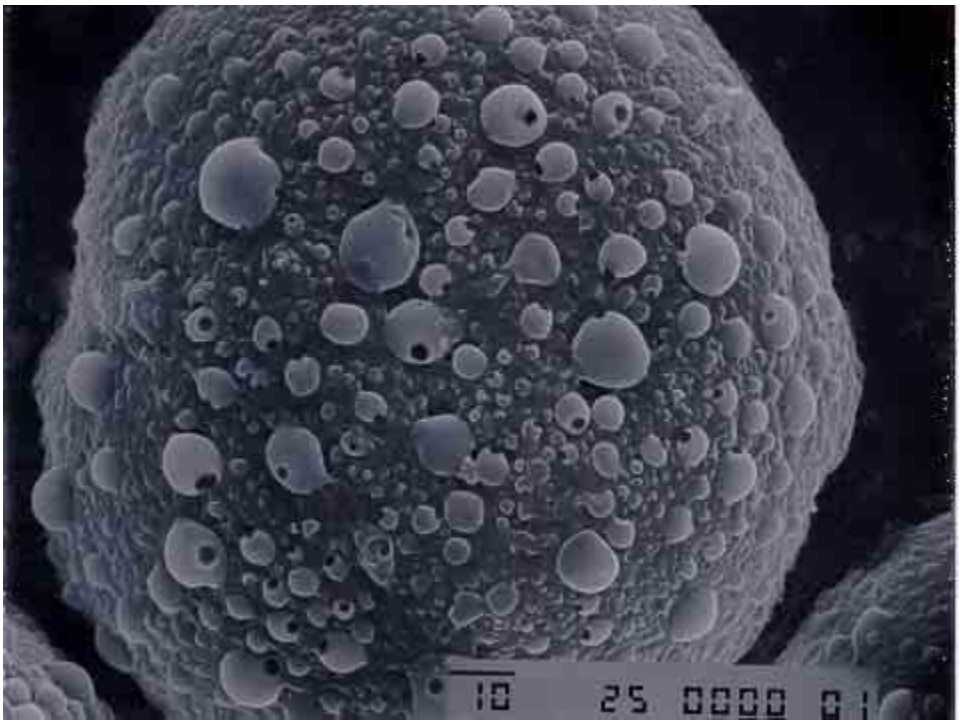

Figure III. An SEM image demonstrating the effective vapor barrier properties of BLOX. This is a sample surface of pure BLOX dissolved with THF and allowed to evaporate. The solvent molecules become trapped and molecules as small as oxygen can form microscopic bubbles that cannot penetrate the surface of BLOX. Shown are secondary bubbles beginning to form.

CHAPTER III

SEM AND OPTICAL MICROSCOPY

Scratches were observed with optical microscopy (Nikon optics from Japan) directly attached to the micro-scratch tester. The eyepiece had a magnification of 10x and scratches were observed using either of two objective lenses – 5x or 20x.

Scanning electron microscopy (SEM) was performed in our laboratory with a Jeol JSM-T300 scanning microscope equipped with a Tracor x-ray analyzer and a Polaroid camera also by Jeol-Technics Co. (Tokyo, Japan). The non-conductive polymer samples were gold plated.

Fouad and Johannesson categorize the coating-substrate response to scratch testing into three regions: "region (I), mild plastic deformation at low applied load up to tensile cracking; region (II), regular and irregular crack patterns at higher load; region (III), coating removal (flaking, buckling, etc.) at increasing load beyond the critical load." [21] Either SEM or optical microscopy may observe these responses. However, according to Hedenqvist and Hogmark, "the most straightforward method for monitoring the scratch test is optical microscopy". [14]

Consider an example of the damages that are caused by very shallow scratching in a material that has low scratch recovery. Liew, Wu, Chow and Lim [22] confirmed by SEM that relatively large surface and subsurface damage from heavy indentation and scratching resulted in large magnetization changes and loss in magnetic recording disks as a result of magnetic recording pattern degradation – an example of what might happen when the recording head in one's personal computer "crashes". The mechanism of magnetization changes is displacement of materials due to the formation of dislocations and cracks in thin film layers. The SEM contrast in the cracks also indicated differences in the exposed materials from the surface (carbon overcoat). Even for the very shallow indent of 200 nm the scanning electron micrograph

revealed a very small indent mark. The magnetic patterns remained relatively intact below very shallow indentations. [22]

Since our fluoropolymers are often flexible, the surface is typically frozen in liquid nitrogen and then fractured. The fractured edge is then positioned vertically and then coated with gold. As noted in a recent LAPOM paper [18], fluoropolymers - such as 12F-PEK synthesized by P. Cassidy at the Southwest Texas State University in San Marcos and from now on referred to as FP-1 - will exhibit a phase inversion at the surface in which the fluoropolymer becomes the matrix; Figure IV.a. This appears as an extensive "honeycomb-like" structure with the epoxy now being located within the "honeycombs". Figures IV.b and IV.c are SEM unfractured surface images of pure FP-1 at the magnifications of 3,500x and 10,000x, respectively. A cavernous structure is apparent in both images of the pure FP-1. As previously discussed, a concentration of only 10 % FP-1 in an epoxy will segregate preferentially to the surface forming a honeycomb matrix of FP-1 with some epoxy dispersed sparingly within the honeycomb matrix at the surface. The cavernous structures of Figures IV.b and IV.c vaguely resemble the honeycomb structure of Figure IV.a. From these SEM images it is apparent that the addition of epoxy causes morphological changes in FP-1 leading to the honeycomb structures shown in Figure IV.a. [18, 19]

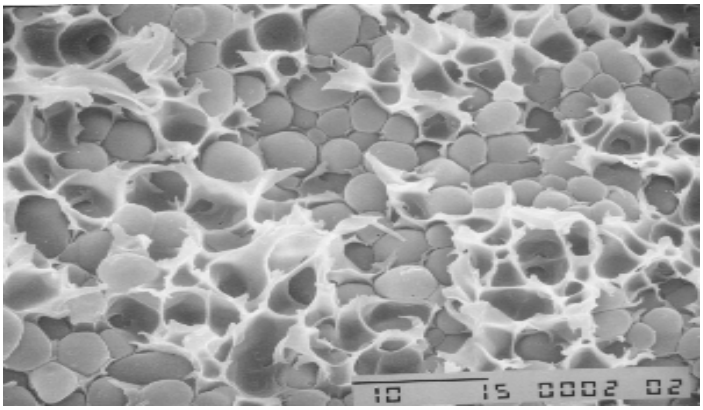

(a)

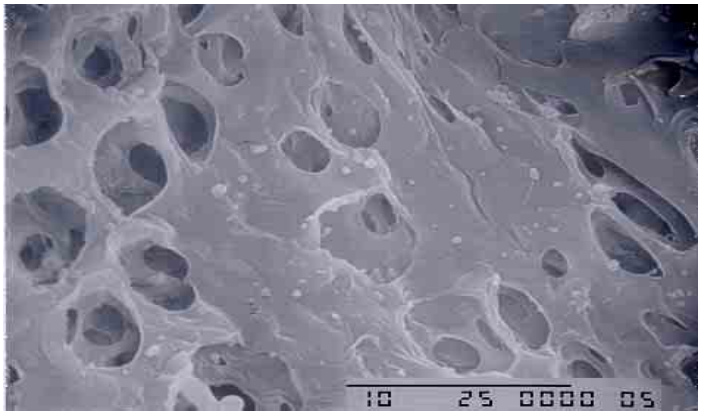

(b)

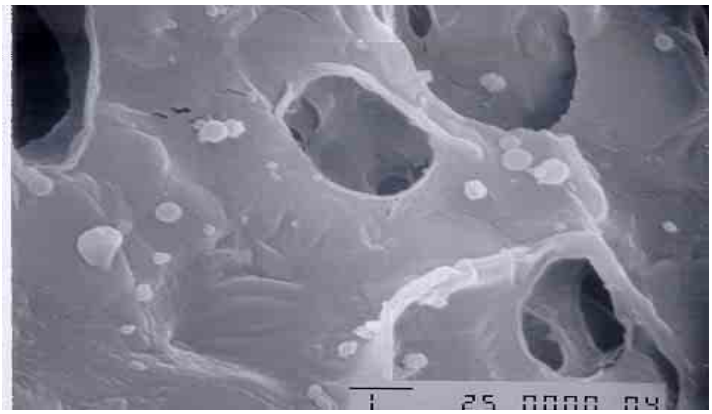

(c)

Figure IV. (a) An SEM image of the top surface of a 30 % fluoropolymer blended with an epoxy. In this case the fluoropolymer is FP-1. A phase inversion has occurred near the surface, with FP-1 becoming the matrix. The small spherical shaped objects located within the honeycombs are epoxy globules. (b) An SEM image of pure FP-1 at the magnification of 3,500x. The morphology is cavernous. This appearance changes to honeycombs when FP-1 is blended with an epoxy. (c) the image shown in (b) at the magnification of 10,000x.

CHAPTER IV

THERMOSETS, THERMOPLASTICS AND MULTIPLE COMPONENT POLYMER SYSTEMS

It is common to divide plastic materials into thermoplastics and thermosets. Thermoplastics are composed of linear or branched polymer molecules with no crosslinking, and for that reason they melt. Thermoplastics are first synthesized and then at a later stage molded. In comparison, thermosets are crosslinked polymers that do not melt. In a thermoset an uncrosslinked prepolymer is given the desired final shape and the polymer is crosslinked at a later stage while it is kept in the mold. [23] BLOX is a hybrid of a thermoplastic and a thermoset.

Basic understanding of how structure variations alter physical and chemical properties helps to transform coatings technology from an art to a science. Coatings chemists have been making this transition for many years. For example, of the previous 42 Mattiello Lectures, at least 10 have dealt with the relationships between the structure and properties of coatings. [24]

The word "structure" is broadly used to describe a material on several levels, from the macroscopic down to the molecular level. Undoubtedly, the chemical structure of a repeating monomer is important. The term "tertiary structure" has been borrowed from the biochemists. Primary structure includes atom to atom connections and the empirical formula; that is, the numbers of each kind of atoms in a compound. Secondary structure gives the relative positions of atoms within individual molecules, and in this context, we refer to conformations of molecules. We could use the term "tertiary structure" to describe how molecules pack together. A term that some may find synonymous is "polymer morphology". The term "morphology" is often used when a material separates into more than one phase whereas tertiary structure applies to molecular packing within a single phase. We cannot explain physical property variations

based on primary and secondary structures alone. [24] Therefore, a thermoplastic and a thermoset have different tertiary structures. Knowing this, one would expect a fluoropolymer such as FP-1 (or FP-4 which was also investigated) to behave differently depending upon whether it is blended with a thermoset or a thermoplastic. While in a thermoset the matrix is crosslinked, in a thermoplastic it is not. In practice, the crosslink density may vary between these two extremes – from heavy crosslinking to no crosslinking.

If an amorphous polymer is crosslinked, the basic properties are fundamentally changed. In some respects the behavior at a high degree of crosslinking is similar to that at a high degree of crystallinity. (Crystallization can be considered as a physical form of crosslinking). The influence of the glass transition temperature becomes less and less pronounced as crosslinking progresses. [25]

Macromolecules are giant molecules in which at least a thousand atoms are linked together by covalent bonds. They may be linear chains as in thermoplastics or three-dimensional networks as in thermosets. [25]

Many natural substances, especially the biological construction materials, are macromolecules. Of these, proteins and cellulose are the most important. While cellulose (being made up of β-D-glucose units) has a relatively simple chemical structure, proteins are built up from many amino acids (varying from four to about twenty-five), in a fixed sequence. This gives the proteins a very marked identity. In some cases the whole protein macromolecule is one single chemical unit, characterized by the nature and sequence of its amino acids. [25]

In contrast with these complex natural macromolecules, many synthetic macromolecules have a relatively simple structure since they consist of identical constitutional repeating units (structural units). This is the reason they are called polymers. If the basic units are identical we

have a homopolymer; if there are more kinds of basic units (e.g. two or three) we have a copolymer. [25] Fluoropolymers are often copolymers as in the case of FP-5 and FP-6.

There are two important characteristics of polymers: their chemical structure (CS) and their molecular mass distribution (MMD) pattern. The chemical structure of a polymer comprises:

a. the nature of the repeating units
b. the nature of the end groups
c. the composition of possible branches and crosslinks
d. the nature of defects in the structural sequence. [25]

The molecular mass distribution informs us about the average molecular size and describes how regular (or irregular) the molecular mass is. The molecular mass distribution may vary greatly, depending on the method of synthesis of the polymer. [25]

These two characteristics, CS and MMD, are believed to determine the properties of the polymer. Van Krevelen [25] argues that these properties determine directly the cohesive forces, the packing density (and potential crystallinity), and the molecular mobility (with phase transitions). In a less direct way they control the morphology and the *relaxation* phenomena. They provide a good approximation for certain purposes to the behavior of a polymer, but it is not exact. [25]

Polymers of a finite size contain so-called end groups that do not form part of the repeating structure. Their effect on the chemical properties cannot be neglected; however, their influence on the physical properties is usually small at the degrees of polymerization actually used in practice. [25]

Every polymer structure can be considered as a summation of structural groups. A long chain may consist mainly of bivalent groups. Any bivalent group may also be replaced by a trivalent or tetravalent group, which in turn carries one or two monovalent groups, thus forming again a

larger molecule of hydrocarbons and non-hydrocarbons known as a "composed" group. Table III gives some of the most important structural groups as defined by van Krevelen. [25]

Polymeric materials consisting of more than one component are produced in increasingly larger quantities and their importance continues to increase. These materials are often stronger and/or tougher than one-component systems. In the field of metallurgy this fact has been known for centuries already: materials many centuries old are found containing metal alloys that are often as well-preserved as the isolated metals themselves. [25] Today, polymer alloys are discovered that are designed to outlive the pure components.

Multi-phase systems in a material may actually impart beneficial properties. Stephen A. Fossey [26] presented a structural description of the intercrystalline polymer interphase based on an atomistic modeling for spider silk fibers. The presence of the interphase is postulated as the origin of the interesting mechanical properties of spider silk. The model postulates a three-phase system, a crystalline phase composed of β-sheets, an amorphous phase and a phase of constrained chains between the crystalline and amorphous phases. It is the constrained chain phase that results in the unusual combination of high initial modulus, strength and toughness. Restated, the three phases are: a large number of very small crystallites, some amorphous regions and an interphase that surrounds the crystalline domains. The amorphous domains are considered rubbery and are arranged as a continuous amorphous matrix with small crystallites imbedded in it. The interphases connect between crystallites and either amorphous domains or other crystallites. The model is consistent with a number of observations of spider silk. [26]

Van Krevelen makes a distinction in polymeric systems based on the nature of the blend of the components. They may be (1) homogeneous on a molecular or a microscopic scale, or (2) heterogeneous on a macroscopic and/or microscopic scale. [25]

Multicomponent polymer systems can be divided into two main classes [25] – see Table IV: (A) Materials containing only polymeric components and (B) Polymer-based systems containing non-polymeric components. Class A systems are subdivided into two subclasses: (A1) Intramolecular blends or copolymers and (A2) intermolecular blends or polymeric alloys. Pure polymer liquid crystals (PLCs), called self-reinforcing polymers, are an example in a homogeneous A1 category. A homogeneous subgroup A2 material is really a homogeneous alloy, in which the components form a single phase. True miscibility is relatively rare; more often we have partial miscibility, usually called compatibility. If a blend contains a compatible rigid component, dispersed with a flexible one at the molecular level, the system is called a molecular composite (which must be well distinguished from the traditional composites.) [25]

Subclass B1 is formed by polymers blended with non-polymeric additives. It can be further distinguished into the subgroup of *plasticized* or "soft" polymers and the subgroup of *filled* polymers. A filler is usually cheaper than the polymeric material, such as carbon black. A filler can constitute as much as 40 % by weight of the material. [25]

Subclass B2 is formed by the so-called *structural composites*, in which a mechanical reinforcement is given to the polymer. Of this subclass the most important are the *fiber-reinforced polymer systems*. The two components, the polymer matrix and the reinforcing fibers or filaments (glass, ceramic, steel, textile, PLCs etc.) perform different functions: the fibrous material carries the load, while the matrix distributes the load – the fibers act as crack stoppers, the matrix as an impact-energy absorber and reinforcement connector. Interfacial bonding between the two is a crucial problem. [25]

If any of the above systems are not at equilibrium then relaxational behavior can be observed. Relaxation is the time-dependent return to equilibrium (or to a new equilibrium) after a

disturbance. Relaxation processes are ubiquituous. They are found in all branches of physics and some examples include: mechanical relaxation (stress and strain relaxation, creep), ultrasonic relaxation, dielectric relaxation, luminescence depolarization and electronic relaxation (fluorescence). Also chemical reactions may be classified under the relaxation phenomena. It will be readily understood that especially in materials science this time-dependent behavior observed in polymer systems is of particular importance. [25]

Table III: Examples of Structural Groups[25]

GROUPS	Monovalent	Bivalent		Trivalent	Tetravalent
1. Hydrocarbon groups	$-CH_3$	$-CH_2-$	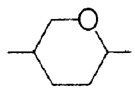	$>CH-$	$-\overset{\vert}{\underset{\vert}{C}}-$
	$-CH=CH_2$	$-CH=CH-$		$-CH=C<$	$>C=C<$
	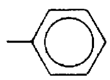	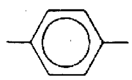	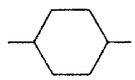	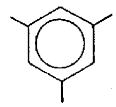	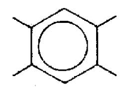
	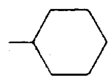	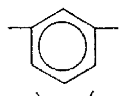	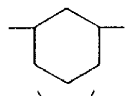		
		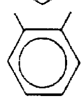	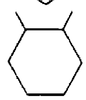		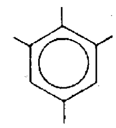
2. Non-hydro-carbon groups	$-OH$	$-O-$			
	$-SH$	$-S-$			
	$-NH_2$	$-NH-$			
	$-F$	$-C(=O)-$		$-N<$	$-\overset{\vert}{\underset{\vert}{Si}}-$
	$-Cl$				
	$-Br$	$-S(=O)_2-$			
	$-I$				
	$-C\equiv N$				
3. Composed groups		$-O-C(=O)-$		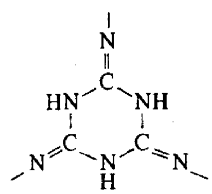	
		$-NH-C(=O)-$			
	$-COOH$	$-O-C(=O)-O-$			
		$-O-C(=O)-NH-$			
		$-NH-C(=O)-NH-$			
	$-CONH_2$	$-C(=O)-O-C(=O)-$			
		$-O-C(=O)-O-C(=O)-O-$			
		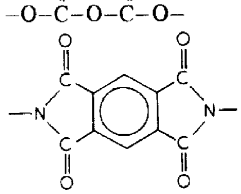			

Table IV: Classification of Multiple Component Polymer Systems[25]

CLASSES	Subclasses	Subgroups	
		Homogeneous (molecular/micro scale)	Heterogeneous (micro/macro scale)
A *Multiple Component Polymeric Materials* (only polymeric components)	A1 *Intramolecular Blends or Copolymers* (alternating, random, block-, graft-, network- or crosslinked)	A11 *(Co)polymers with rigid segments* or pure *polymeric liquid crystals* (self-reinforcing)	A12 Block-copolymers with large difference In glass transition between components
	A2 *Intermolecular Blends* or *Polymer Alloys*	A21 Homogeneous polymer Alloys *Molecular composites* (if one component rigid)	A22 *Heterogeneous Polymer alloys* (e.g., rubber particles)
B Polymer-based Systems (often containing non-polymeric components)	B1 Polymers with *non-polymeric added materials (Functional Composites)*	B11 *Plasticized polymers* (e.g. plasticized PVC)	B12 *Filled polymers* (Fillers: silica, talc, carbon black)
	B2 Reinforced Polymers *(Structural Composites)*	B21 Blends of polymer with compatible anti-plasticizer	B22 *Fiber-reinforced Polymer systems* (Fiber or filament: carbon, glass, steel, textile, PLCs)

CHAPTER V

SAMPLE PREPARATION

V.1. Thermoset blends

Fluoropolymers coded as FP-1, FP-2, FP-3 and FP-4 were synthesized in the Department of Chemistry at Southwest Texas State University. The epoxy used was a diglycidyl ether of bisphenol A resin (Shell Chemicals – EPON^{TM} 828) cured with an aliphatic amine (triethylenetetramine TETA – Shell Chemicals – EPI-CURE^{TM} 3234). Chemical structures are not shown due to proprietary reasons.

The sample preparation procedure for FP-1 is as outlined in Brostow et al. [18] The system was cured at 24ºC and 70ºC. The fluoropolymer was dissolved in acetone (20 ml acetone/1 g FP-1) and then the epoxy resin was added. The mixture was completely miscible. The curing agent was then added according to the producer specifications (13 g curing agent/100 g epoxy). Samples containing from 5 to 50 weight % of FP-1 in the final system, epoxy + FP-1 + curing agent, were prepared. One half of the mixture was cured at 70ºC for 3 hours and the other half was cured at 24ºC for one week in order to simulate room temperature curing applications. The samples were stored at 24ºC.

FP-2 would not completely dissolve in 100 % acetone; therefore, a mixture of 30 % THF + 70 % acetone was necessary while gently heating the mixture to 30ºC. Samples were prepared containing from 5 to 50 weight % of FP-2 in the final system, epoxy + FP-2 + curing agent although we discovered there is no advantage to increasing the fluoropolymer concentration above 20 weight %. 20 ml of the 30 % THF + 70 % acetone solution was added for each 2.4 grams of total mixture (FP-2 + epoxy + curing agent). The fluoropolymer was dissolved first, the epoxy was added and then the curing agent was mixed thoroughly into the solution. One half of

this mixture was cured at 70ºC for 3 hours and the other half was cured at 24ºC for one week in order to simulate room temperature curing applications. When completely dry, the samples had a thickness of 500-600 microns with a surface area of approximately 19.63 cm^2 – the bottom area of the aluminum sample pans. These were cut into approximately 1 cm^2 segments for scratch testing.

FP-3 will dissolve in 100 % acetone; however, it will completely dissolve only very slowly. 25 ml acetone/0.5 g of FP-3 were necessary to dissolve this fluoropolymer. Otherwise, the sample preparation was essentially the same as for FP-1. The system was cured at 24ºC and 70ºC. The fluoropolymer was dissolved in acetone and then the epoxy resin was added. The curing agent was then added (13 g curing agent/100 g epoxy). Samples containing from 0 to 20 weight % of FP-3 in the final system, epoxy + FP-3 + curing agent, were prepared.

FP-4 would not completely dissolve in 100 % acetone; therefore, a mixture of 10 % THF + 90 % acetone was necessary – similar to the FP-2 procedure. First the fluoropolymer was dissolved, the epoxy was added and then the curing agent was mixed in as outlined for FP-2. 20 ml of the 10 % THF + 90 % acetone solution was added to each 2.4 grams of total mixture (epoxy + FP-4 + curing agent).

V.2. Thermoplastic blends – solvent method and non-solvent method

V.2.a. The solvent method

FP-7 was blended with pulverized BLOX pellets. The pulverization technique involved freezing the BLOX pellets in liquid nitrogen for 10 minutes and then pulverizing the frozen pellets for 5-10 minutes. The fragmented pellets were then frozen again and re-pulverized – this was repeated at least two more times until a fine powder was achieved. Samples containing from

5 to 50 % FP-7 by weight in the final system, BLOX + FP-7, were prepared. The combined total weight of BLOX + FP-7 was 2.4 grams in each sample. In each case, the pulverized BLOX was allowed to dissolve in approximately 20 ml of THF with constant stirring for at least 6 hours at room temperature – the beaker was covered with aluminum foil to prevent evaporation. Then the FP-7 was added to the solution with constant stirring until dissolved. The mixture was poured into an aluminum pan and allowed to cure at room temperature for 1 week (although a teflon mold was later shown easier to use). Also, a pure BLOX sample was prepared by dissolving 2.4 grams of pulverized BLOX in 20 ml of THF and a pure FP-7 sample was prepared by dissolving 2.4 grams of FP-7 in 20 ml of THF for comparison purposes. The complexity of this sample preparation was facilitated by the Taguchi method – an L4 array was designed listing possible combinations of sample preparation procedures. [20]

V.2.b. The non-solvent method

Pulverization of BLOX was the same as outlined for the solvent method. Materials developed for a different project coded as LB-22 and PLC-3 were also pulverized in the same manner. PLC-3 is a polymer liquid crystal. Samples containing from 0 to 20 % LB-22 by weight in the final system, BLOX + LB-22, were prepared. The combined total weight of BLOX + LB-22 was 4.0 grams in each sample. The same sample preparation technique was applied to PLC-3 + BLOX blends. No solvents were used. Instead the samples were placed in a vacuum oven at 155°C for 4 hours. Two sets of samples were prepared for LB-22 and PLC-3 at 155°C – one at atmospheric pressure (30.2 inches of Hg) and the other under vacuum (20 inches of Hg).

CHAPTER VI

RESULTS FOR EPOXY + FLUOROPOLYMER BINARY SYSTEMS

VI.1. The purpose of the epoxy resin

Carlsson, Bexell and Olsson [27] state that the main purpose of the resin in a permanent coating is to hold the additives on the surface and so the resin itself does not need intrinsic functional properties. They declare, however, the resin material should have a sufficient load carrying capacity, chemical resistance, hardness and wear resistance. [27] This thesis proposes that if this were true then the majority component in the fluoropolymer blend, i.e. the epoxy resin (matrix), is not being used to its full functional capacity! Why not design a matrix that is cheap to make, already has some good scratch recovery abilities and blends well with a fluoropolymer, the expensive minority component, therefore increasing these scratch recovery capabilities even further?

Resins may be organic or inorganic or combinations of these. Fossey and Tripathy mixed coatings known to have good tribological properties with acrylic + polyurethane + polyester resins or polyester + melamine resins. Thin organic permanent coatings tend to loose their good tribological properties with increasing acrylic resin content. [26] Our research also suggests that although our epoxy resin shows fair scratch resistance, a judicious choice of fluoropolymer will increase scratch resistance further. [19]

The fluoropolymers under investigation are binary epoxy blends containing in turn FP-1, FP-2, FP-3 and FP-4. It is important to note that all these fluoropolymers consist of monomer chains that contain a precise amount of carbonyls and benzene ring-like structures known as phenylenes. It will be shown that these groups are just as important in improving scratch depth recovery as the fluorine atoms. More emphasis will be placed upon FP-1 than the other

fluoropolymers since it demonstrated the highest scratch recovery, namely consistently above 90 %. This thesis will also answer the question "Is more better?" – does one improve scratch depth and recovery just by increasing the weight percent of fluorine atoms in the molecule?

At this point the importance of the fluorine atom deserves some attention. Pure fluorine at room temperature is normally a gas. It has the density of 1.58 g/liter and the boiling point of – 188.1º C. A single fluorine atom has a valence shell of 7 electrons until it bonds with another fluorine atom to form F_2 and complete its valence shell with 8 electrons. What is most peculiar about fluorine is that it is highly *electronegative* like oxygen and chlorine. In combining fluorine with a polymer molecule the fluorine atom will bond to a primary carbon through a single bond. By comparison, an oxygen atom may bond to the molecule through a double bond or two single bonds. In either case, fluorine and oxygen are both electronegative.

As noted in two papers from LAPOM [18,19], successful fluoropolymers are characterized by the amount of fluoropolymer segregating to the surface - exactly where friction and scratching will occur. The fluoropolymer sample must be roughly 500 – 600 microns thick in order to handle scratches from the very light forces of 0.03 N to the heavier applied forces above 15 N. The surface must exhibit toughness and a very substantial amount of recovery. Typically, the fluoropolymer is blended with an epoxy in concentrations of 20 % or less since it would be economically unfeasible in most cases to add more than that.

VI.2. Penetration depths

The depths were determined as described in Section 2 of Chapter II. The penetration depth of the scratch was plotted versus the force in Newtons. The same plot was performed for the residual depth. We have results for samples cured at two temperatures; hence we display direct

experimental results for one of them. In Figure V we show curves of the penetration depth as a function of the force applied in the progressive mode for several fluoropolymer concentrations for samples cured at 70˚C. The curves for the samples cured at 24˚C are similar.

We see in Figure V that the addition of the fluoropolymer to the epoxy causes first a decrease and then an increase in the penetration depth. To understand the phenomenon involved, we have created plots of the penetration depth versus concentration of FP-1 for several forces; see Figure VI. The curves in Figure VI as well as in all later Figures of depth versus concentration of FP represent 4^{th} degree polynomials with the parameters determined by a least squares procedure.

We see in Figure VI that the initial addition of the fluoropolymer to the epoxy causes first a certain but not very significant lowering of the penetration depth. We know from the scanning electron micrographs that the fluoropolymer comes preferentially to the surface and attempts to produce the phase inversion even at low concentrations. Before the phase inversion occurs, the diamond indenter tip encounters more or less alternating regions of both phases. This makes the penetration more difficult and the depth decreases along with increasing fluoropolymer concentration. The effect is not large since the curing reaction interferes with the travel of the fluoropolymer towards the surface. [18]

Later on, when more FP-1 is added, the phase inversion begins. Our FP-1 + epoxy at the surface apparently provides a softer surface; the penetration depth begins to increase starting at 10 % fluoropolymer or so, tending towards a maximum or a plateau. After the maximum the penetration depth gradually decreases again (not shown). The surface layer has more cohesion.

Consider in turn the penetration depths for samples cured at 24˚C. For brevity we do not include the depth vs. force curves. In Figure VII we show a plot corresponding to that in Figure VI. There is a significant drop of the penetration depth upon addition of only 5 % fluoropolymer

for all forces except the lowest one indicated. That lowest force necessarily affects the surface the least, the depths for all fluoropolymer concentrations at 2 N are significantly lower than the depths resulting from forces equal to or greater than 4 N. As reported in [18] the phase inversion occurs earlier at 24˚C – and this fact is reflected by increases of the curves for various forces towards maxima at lower fluoropolymer concentrations than for samples cured at 70˚C. At still higher fluoropolymer concentrations the surface layer has more cohesion, the penetration depth decreases.

The significant lowering of the penetration depth at 5 % can be explained by the fact that at 24˚C the migration of fluoropolymer towards the surface is *not* hindered by simultaneous fast curing. It is due to this phenomenon that we achieve the desired result.

VI.3. Residual depths and percent recovery

The fact noted in Chapter II, Section II, that our materials are viscoelastic is pertinent. The penetration depth is also a function of *time*, the recovery is actually quite quick and takes less than 5 minutes. In Figure VIII we show the curves of the residual depth as a function of the fluoropolymer concentration for a number of values of the applied force for FP-1 samples cured at 70˚C. Starting from the pure epoxy, the curves show first minima then maxima. Thus, the results are similar to the original penetration depths – for analogous reasons. When we compare Figures VI and VIII quantitatively rather than qualitatively, we see that the strong recovery occurs in all cases.

To have a measure of the healing that took place, we define the percentage recovery as

$$f = (1 - R_h/R_p) \bullet 100\ \% \qquad (7)$$

where f is the fractional recovery in percent, R_p is the original penetration depth while R_h is the depth after healing. In Figure IX we show the f values calculated from Eq. (7) for a number of concentrations of FP-1. The curves were calculated by applying this equation at each applied force. In most cases the dependence on the applied force is only weak. The 5 % fluoropolymer concentration is an exception: higher applied forces provide first an *increase* in the recovery, a desirable result; later on a plateau is reached. We recall the minima in the penetration depth also around 5 % fluoropolymer in Figure VI.

Figure X is an analogy of Figure VIII, but for samples cured at 24˚C. We observe strong minima first for low fluoropolymer concentrations, followed by maxima. The minima occur at lower fluoropolymer concentrations than in Figure VIII. The explanation is again the earlier and unhindered phase inversion at the lower temperature. The higher the applied force, the more pronounced the minimum at 5 % FP-1.

VI.4. Relation to mechanical properties

Let us now connect the present values to mechanical testing results reported in Brostow et al. [18] A plot of the flexural modulus versus the concentration of FP-1 shows a minimum at about 1.1 GPa (1.1×10^9 N/m^2) in the flexural modulus slightly above 5 % FP-1. The area A of the spherical diamond tip in contact with the sample can be represented by the standard equation for a partial area of the outer surface of a sphere, $A = 2\pi \bullet r \bullet h$; substituting the height h by R_h, we obtain

$$A = 2\pi \bullet r \bullet R_h \qquad (8)$$

where r is the radius of the indenter and R_h as before is the *recovery depth after healing*. Using the results obtained from scratch testing at the concentration of 5 % FP-1, the applied force of

2 N, and the residual depth of 4.30 microns, the area becomes $5.40 \bullet 10^{-9}$ m^2 and the stress becomes 0.37 GPa. However, at this level of force less than half of the indenter seems to be causing the stress (we recall that we also apply stresses twice as large). To get a numerical value, assume that 40 % of the indenter creates the stress. Our estimate gives us now 0.93 GPa. This result is comparable to the flexural modulus of 1.1 GPa [18], an altogether satisfactory agreement given the assumptions made and the different techniques used.

Figure XI shows friction test results for FP-4 in epoxy at various concentrations and cured at 70˚C indicating two areas with minimal values in the curves for both the static and dynamic friction – one at about 3 % and the other at around an 18 % concentration of FP-4. Our Sintech 2 friction table has a margin of error $\pm$ 1/2 % of the frictional reading. The 18 % minimal value for the friction results corresponds well with the 15 % minimum indicated by scratch testing. Both the static and dynamic friction are indicated in the graph for the top and bottom surfaces of the samples. The friction for the top surface of the FP-4 + epoxy samples is substantially lower than the friction for the bottom surface. The explanation is that the fluoropolymer goes preferentially to the top rather than the bottom surface. The epoxy forms extensive crosslinking, and this drives the fluoropolymer to the surface. It is seldom that two different polymers will be completely miscible, and it is believed that differences in densities between the epoxy and the fluoropolymer help to determine whether the fluoropolymer will go to the top or bottom surface. If the densities are similar then the fluoropolymer may be driven to both surfaces.

VI.5. Micro-Scratch Test (MST) Results for FP-2 + epoxy, FP-3 + epoxy, FP-4 + epoxy vs. FP-1 + epoxy

We have shown above [19] that significant increases in scratch depth recovery can be obtained by adding a few percent of FP-1 to an epoxy. The success in scratch recovery of FP-1 led to the investigation of other epoxy + fluoropolymer pairs. As in the previous Section, a minimum in the residual depth versus percent fluoropolymer at various applied forces was also discovered for FP-2, FP-3 and FP-4; see Figures XII – XIV.

FP-2 and FP-4 both show a minimum around 15 % - see Figures XII and XIII. While FP-3 clearly shows a minimum around 5.5 % as indicated in Figure XIV – this graph only shows data up to 10 % FP-3 since our indenter was reaching the substrate for the 15 % FP-3 sample. The minimum of FP-3 compares nicely to the minimum of FP-1 previously shown in Figure VIII; however, FP-1's mimimum is not so clearly defined – we know that for FP-1 cured at 70˚C that the minimum lies near 5 % or greater at lower applied forces. The minimum is clearly at 5 % for the higher applied forces approaching 12 N.

The depth versus force curves for FP-2 and FP-3 were somewhat - though not entirely disappointing and these graphs are not shown. Samples demonstrated relatively poor recovery as compared to FP-1 and FP-4. The percent recovery of FP-4 versus applied force is shown in Figure XV. The results suggest that FP-4 may be segregating to both the top and bottom of the sample starting at concentrations as low as 5 % fluoropolymer addition. The scratch recovery at applied forces below 5 N is above 90 % when the bottom of the sample is scratched and decreases steadily with increasing applied force. In comparison, a 15 % FP-4 addition shows a percent recovery that is stable around 87 % independent of the applied force. As previously

mentioned, a minimum at around 15 % is also seen in a plot of friction versus percent FP-4 cured at 70˚C.

The results for FP-1 and FP-4 at concentrations of 10 % are shown in Figure XVI. The amount of scratch recovery is highly dependent upon the curing temperature and the material. FP-1 demonstrated higher scratch recovery when cured at 24˚C while FP-4 had higher scratch recovery when cured at 70˚C. These results are compared to an epoxy cured at 24˚C that also gave better scratch recovery when cured at room temperature. The percent recovery of 10 % FP-4 (70˚C) is similar to the pure epoxy (24˚C); however, 10 % FP-1 (24˚C) demonstrates a scratch recovery consistently above 90 %.

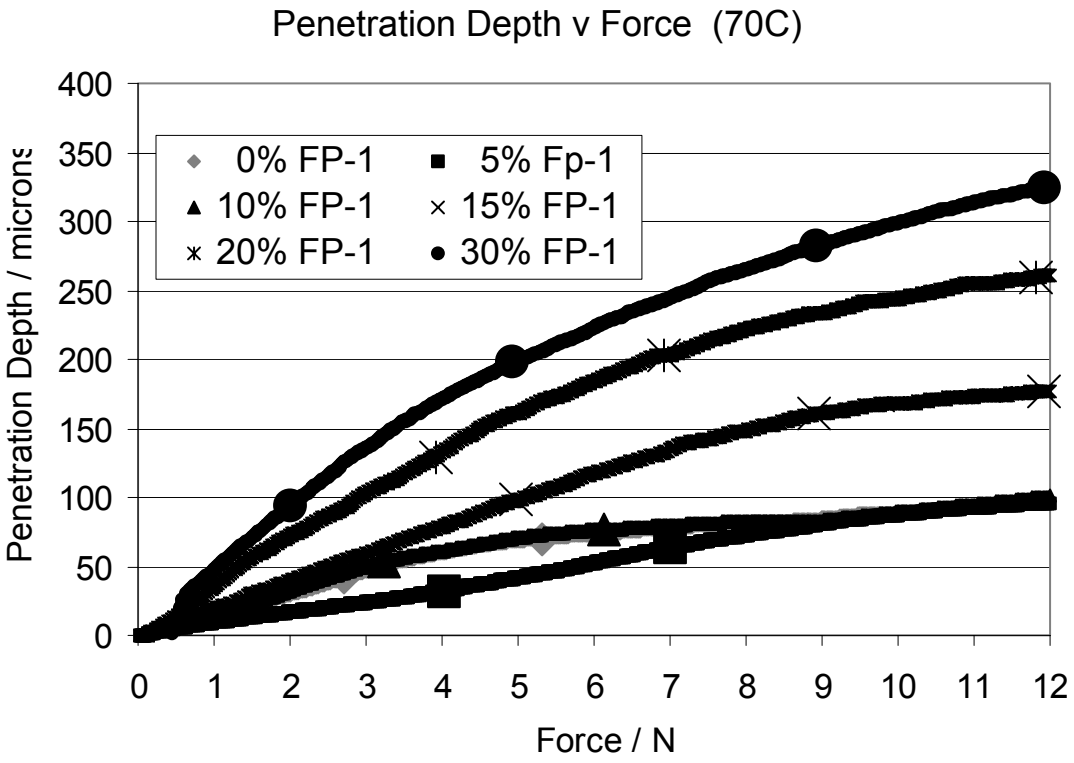

Figure V. The penetration depth as a function of the applied force for several concentrations of FP-1 in the epoxy cured at 70˚C. Each of the plots on this graph is the result of over 800 data points, and represents the average of at least 10 scratches. The margin of error for each of these points is $\pm$ 7.5 nm. The pure epoxy has a relatively low penetration depth, however, this is improved with the addition of only 5 % FP-1 – the penetration depth decreases.

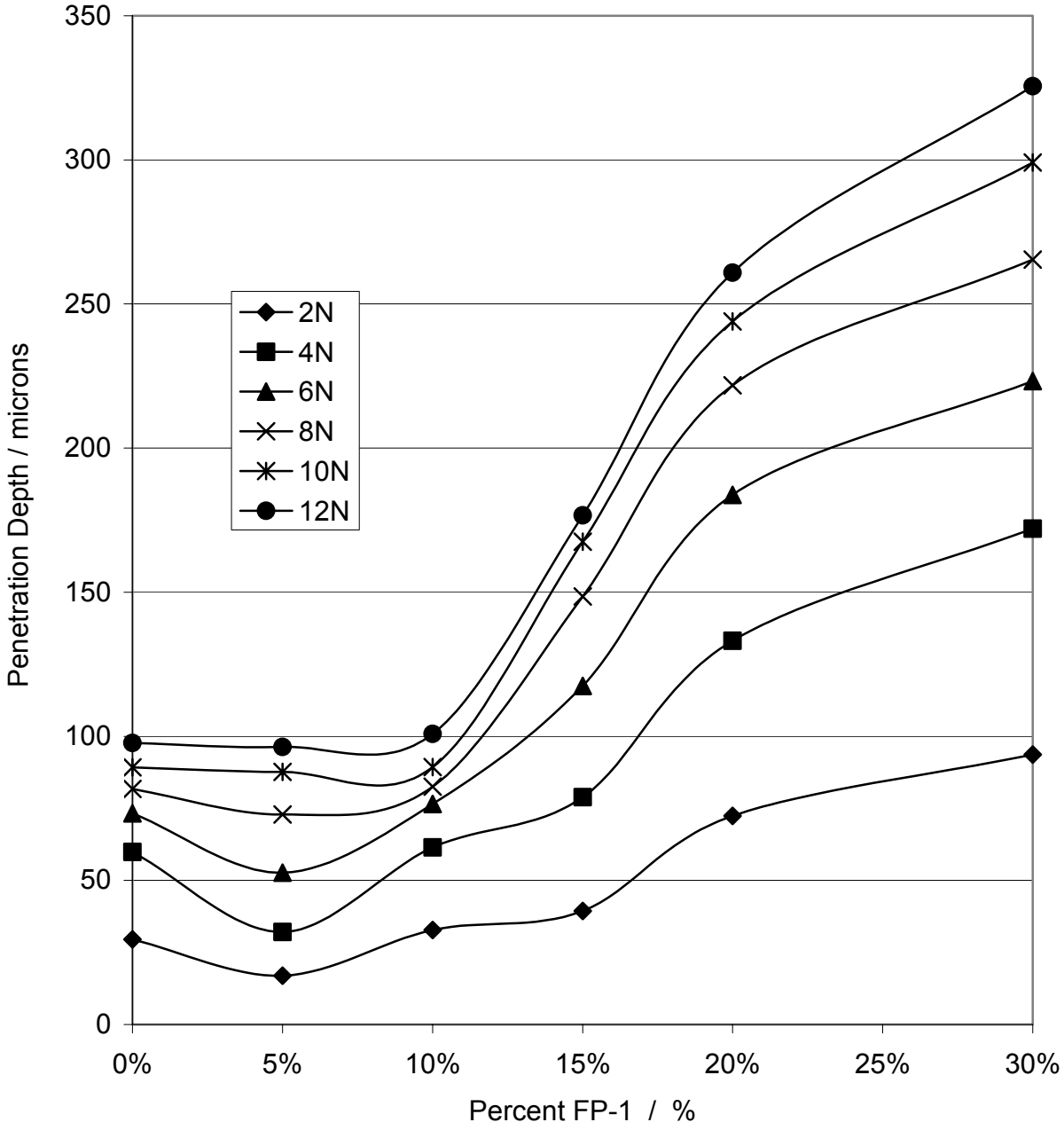

Figure VI. Penetration Depth v Percent FP-1 (70C)

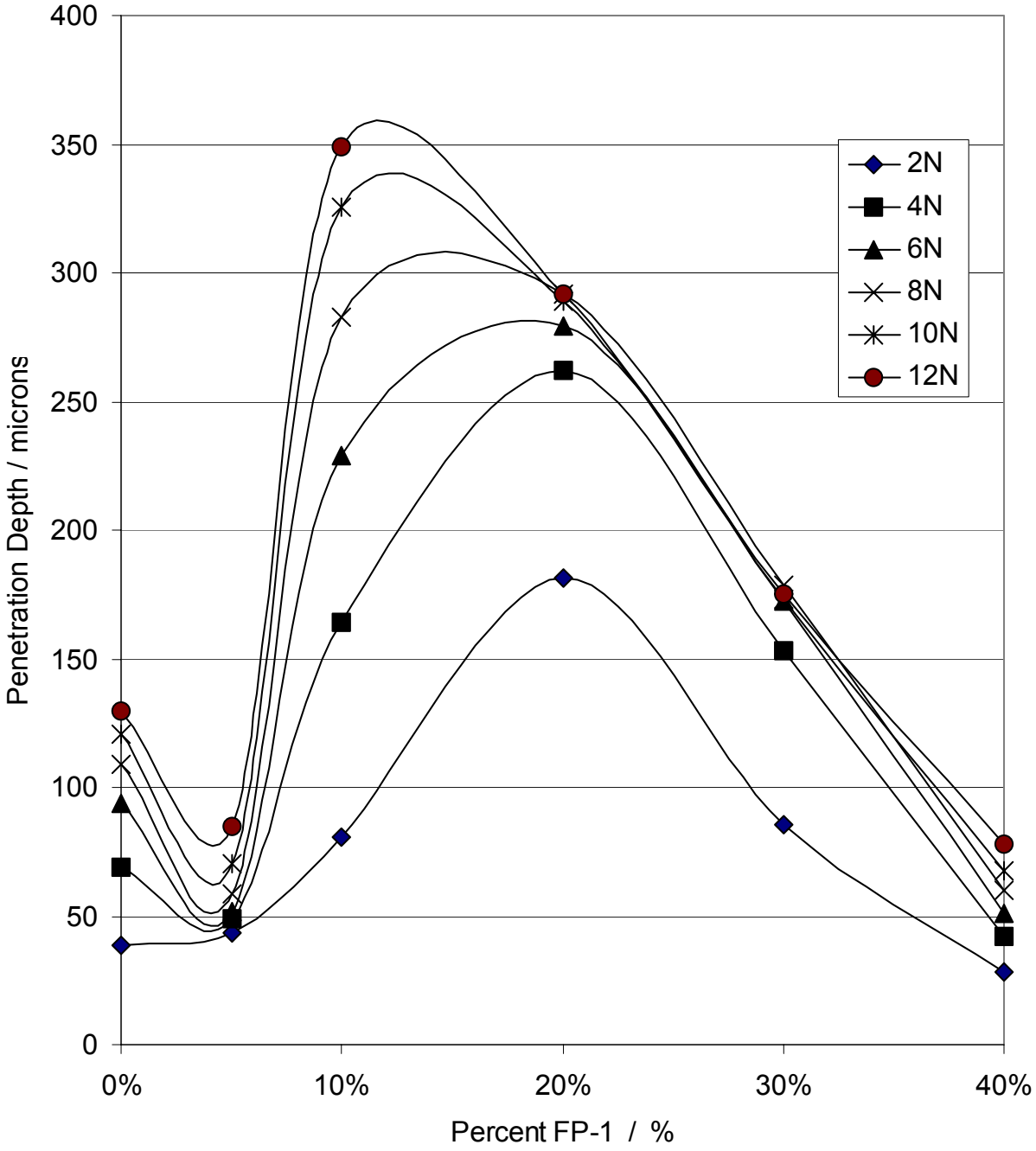

Figure VII. Penetration Depth v Percent FP-1 (24C)

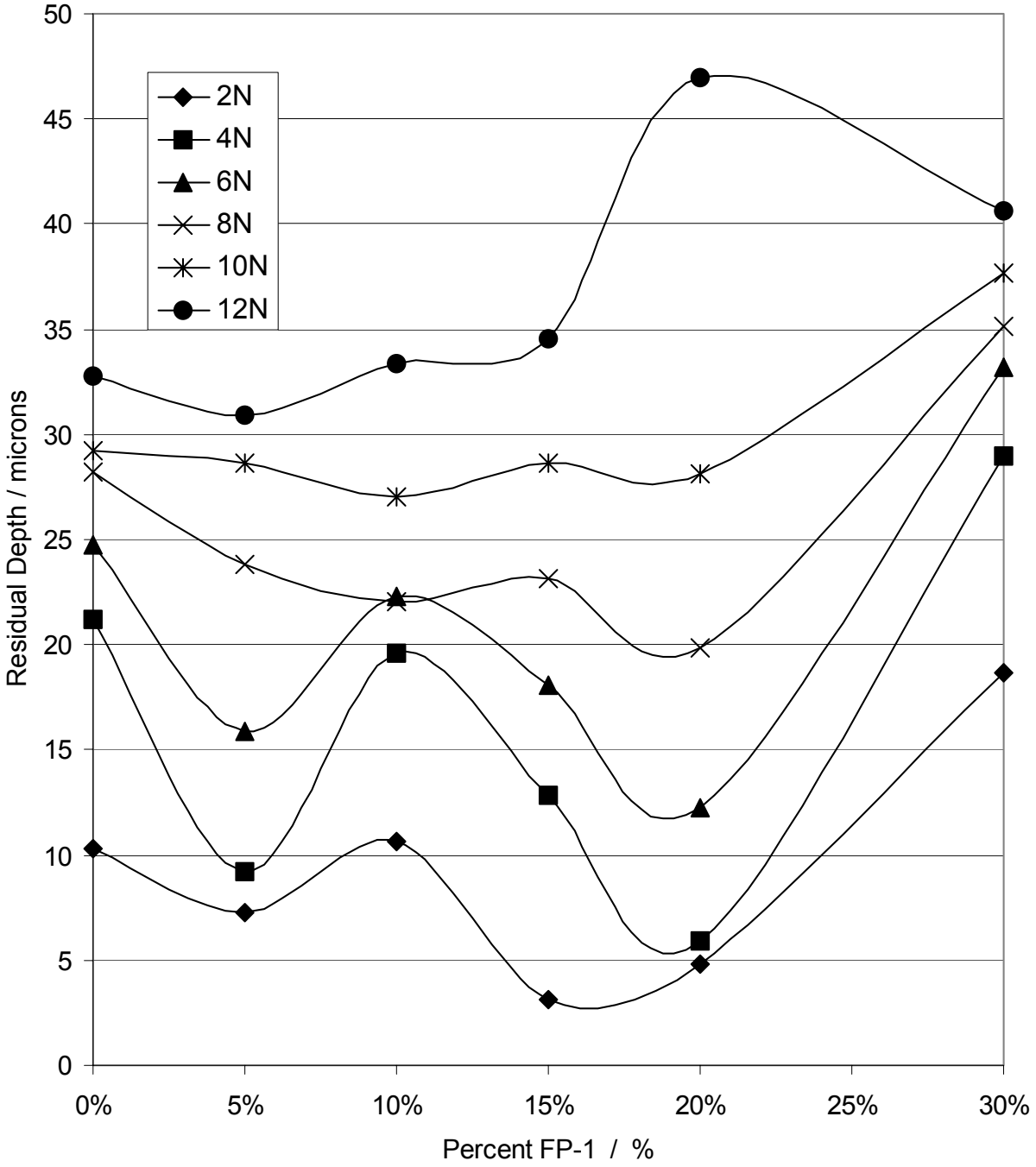

Figure VIII. Residual Depth v Percent FP-1 (70C)

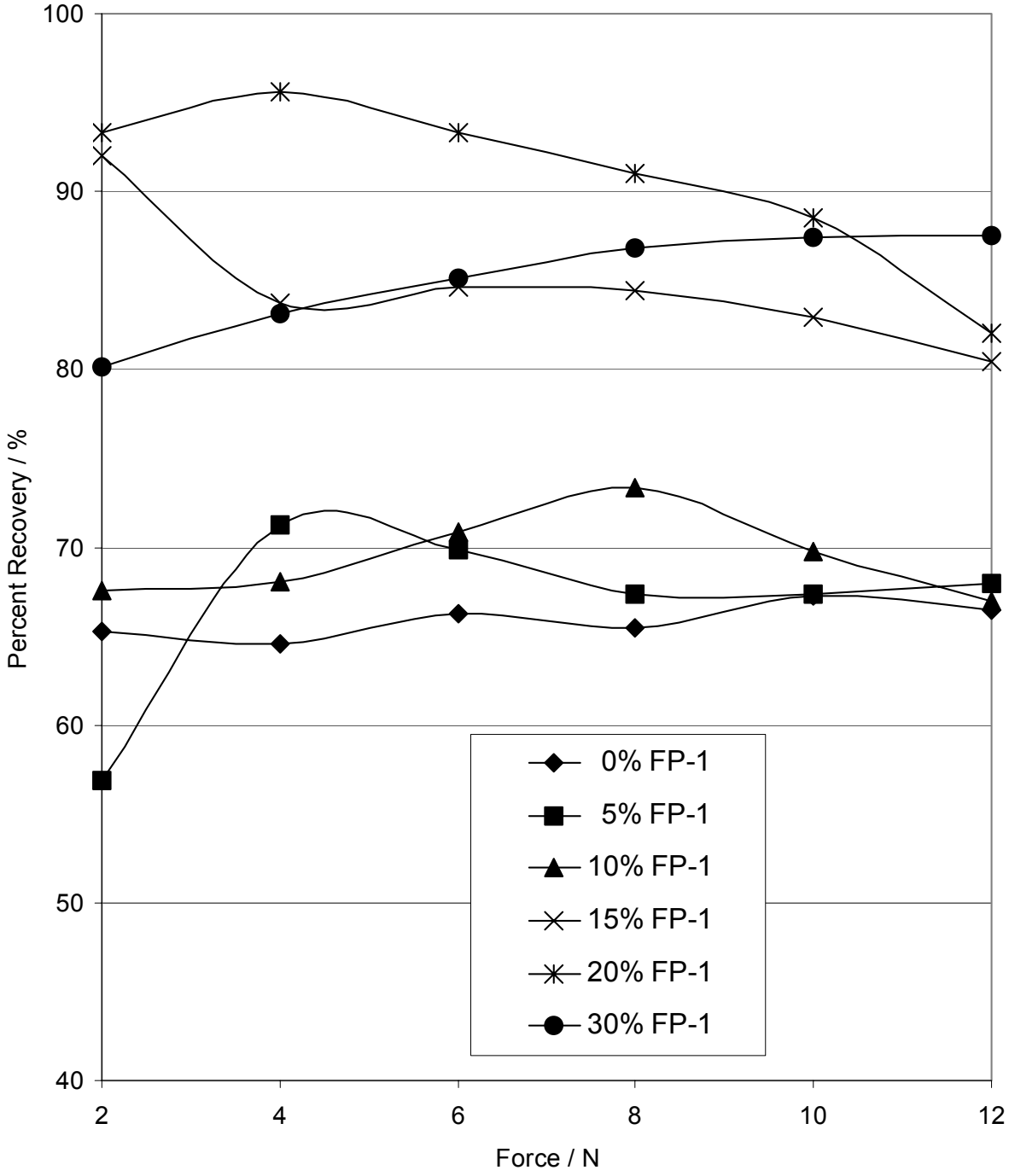

Figure IX. Percent Recovery of FP-1 v Force (70C)

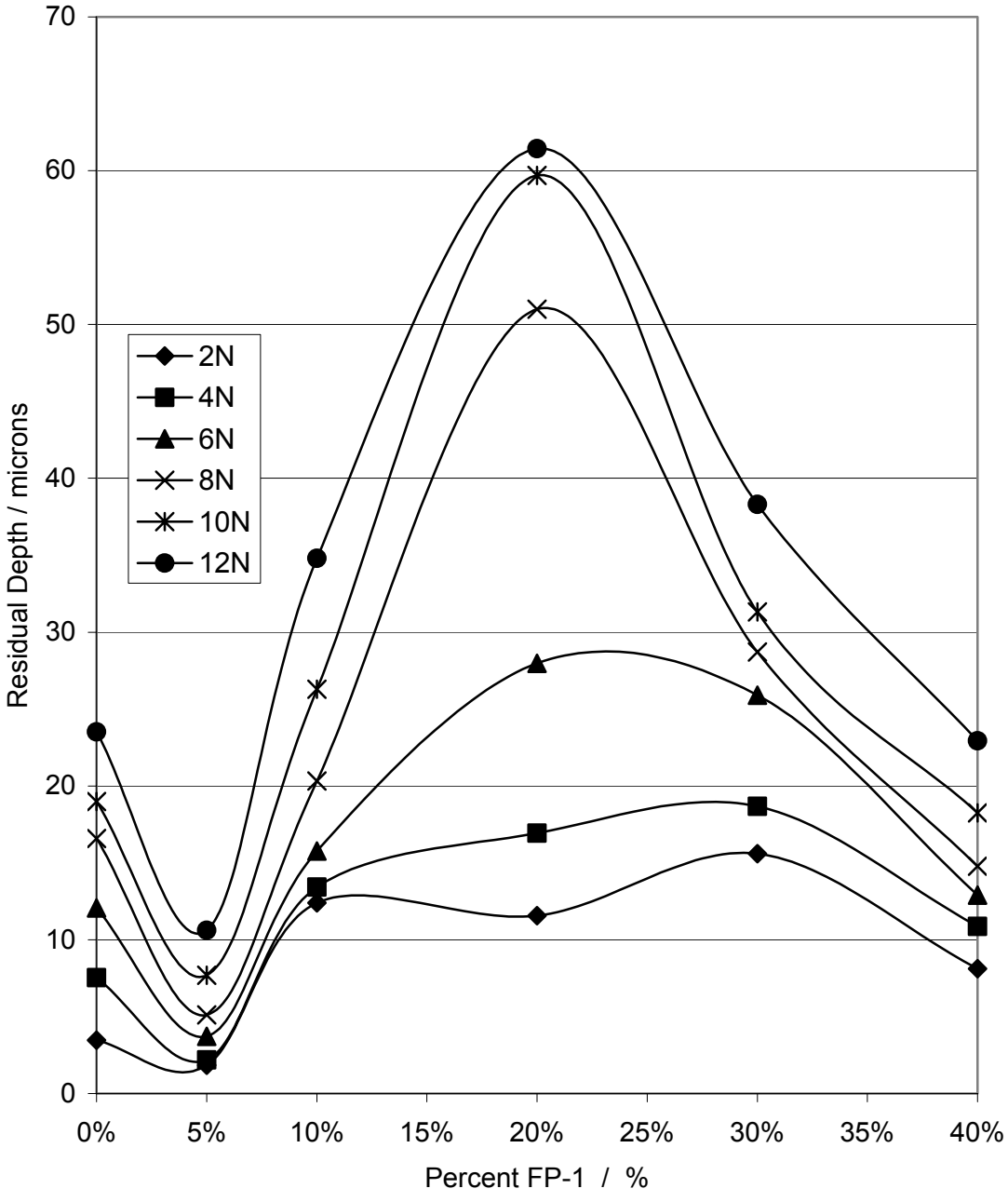

Figure X. Residual Depth v Percent FP-1 (24C)

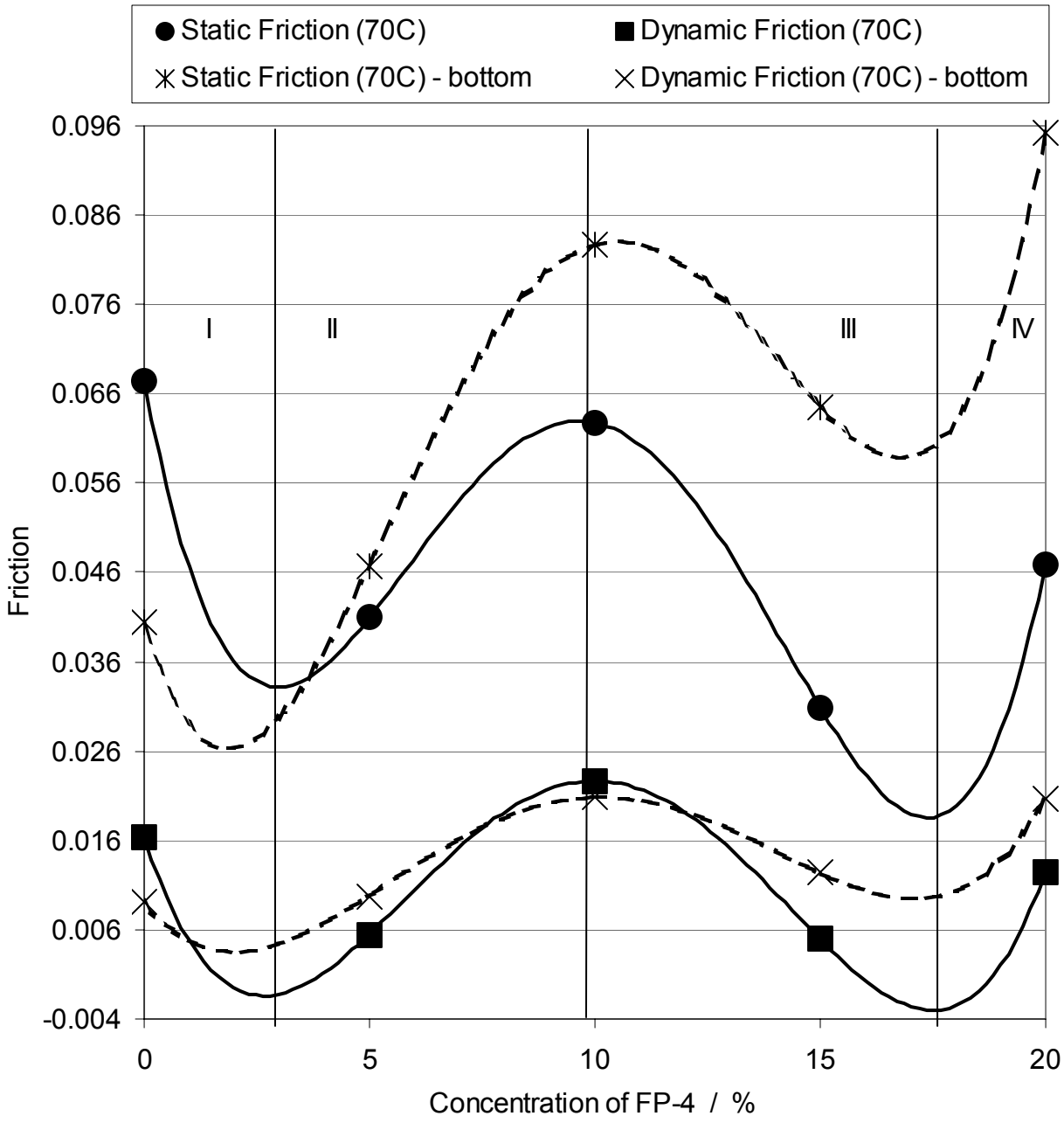

Figure XI. Friction for FP-4 + epoxy blends

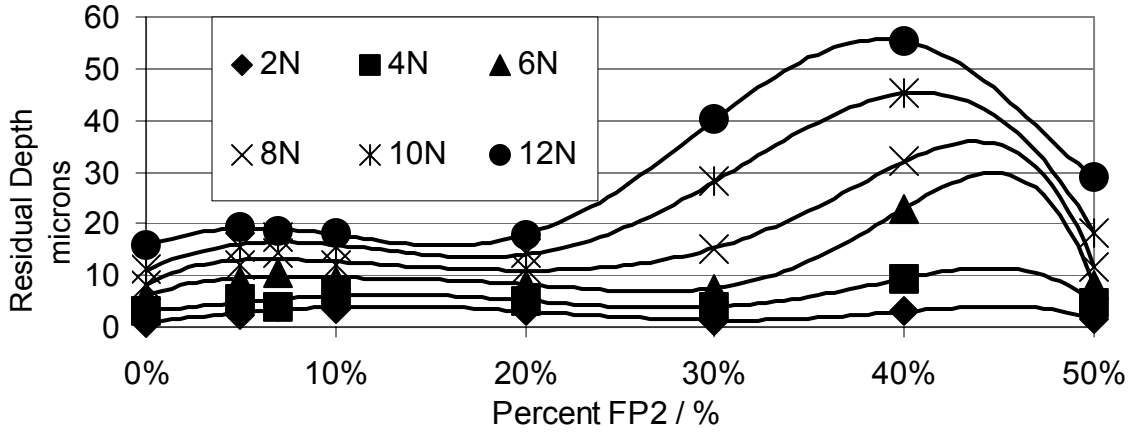

Figure XII. Residual Depth v Percent FP-2 (70C)

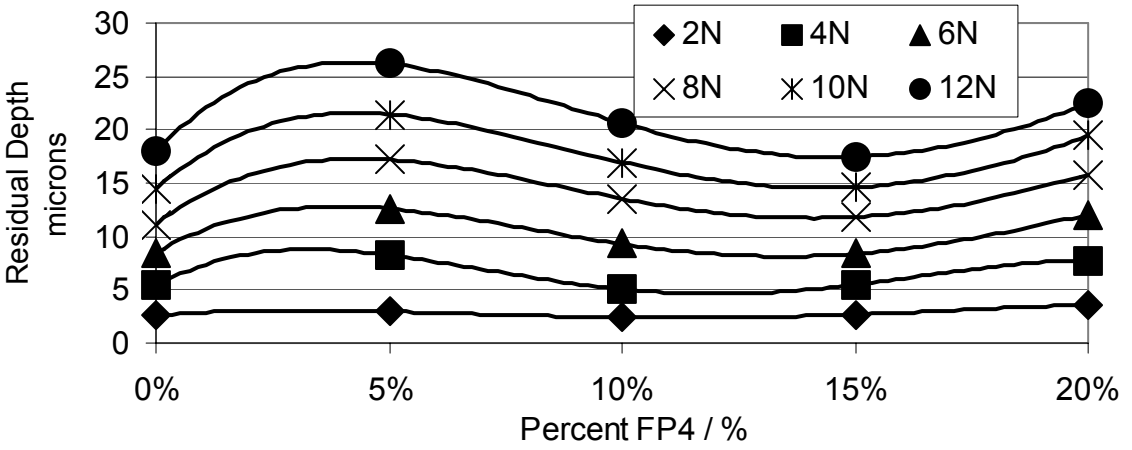

Figure XIII. Residual Depth v Percent FP-4 (70C)

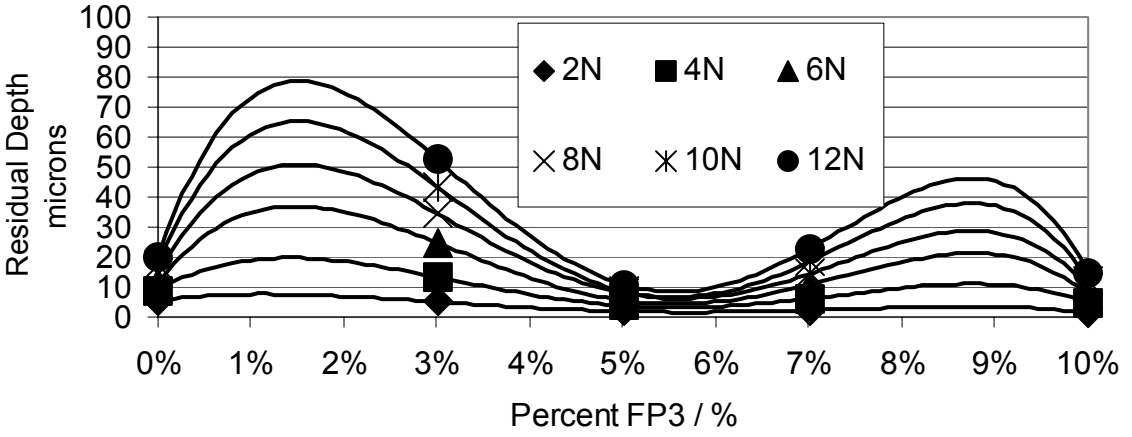

Figure XIV. Residual Depth v Percent FP-3 (70C)

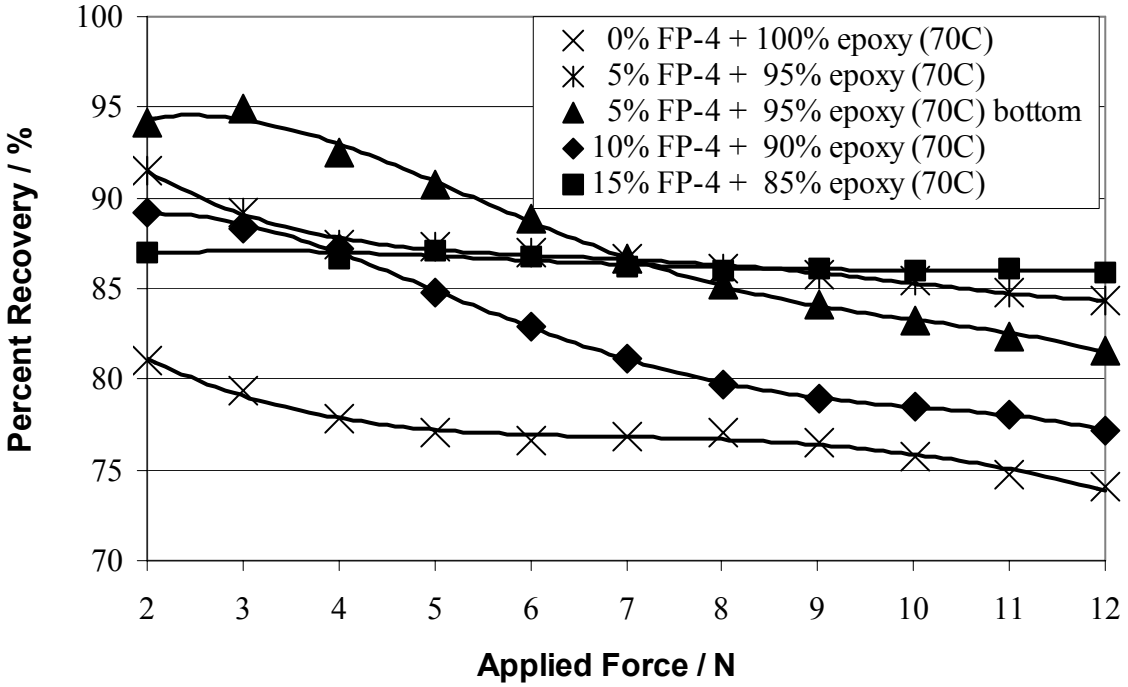

Figure XV. Percent Recovery of FP-4 versus the applied force. The curing temperature was 70C.

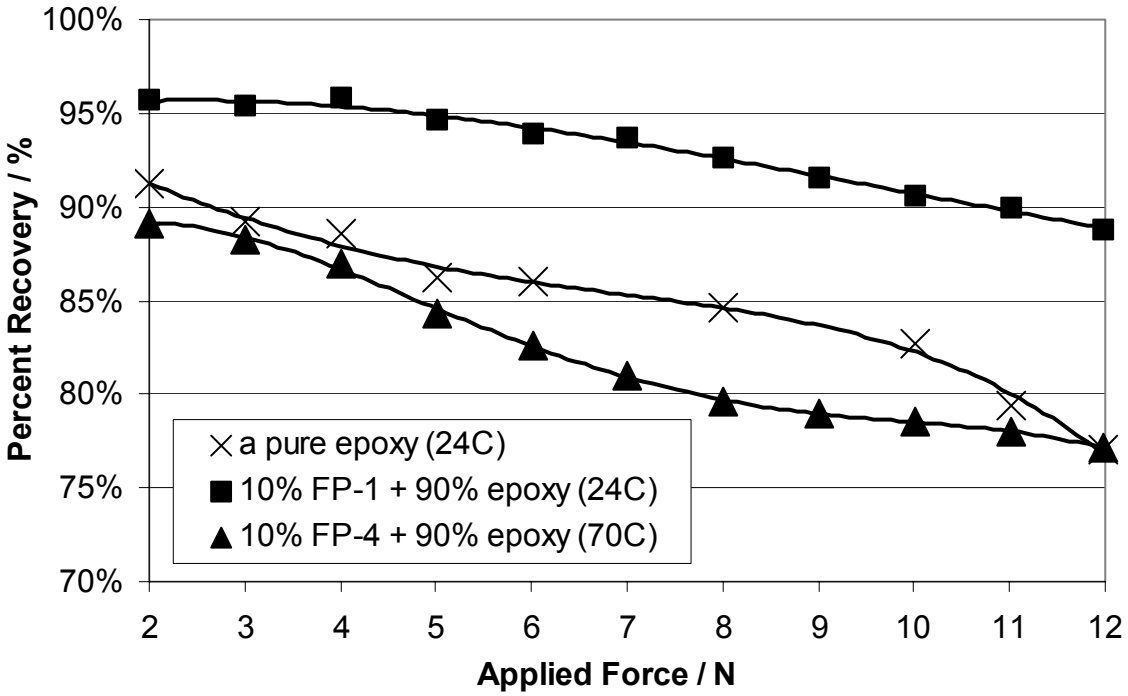

Figure XVI. Percent recovery of FP-1 and FP-4 versus the applied force. Each is represented by its curing temperature that indicated its highest recovery.

CHAPTER VII

THERMOPLASTICS RESULTS

VII.1. Adhesion and failure mechanisms

Ashrafizadeh [28] observes that "...a coating with better mechanical properties and good ductility has the highest load-bearing capacity. It is clearly seen that thicker coatings have a higher load bearing than the thinner ones; however, thick layers...have *lower adhesion* compared to corresponding thinner films." [28] In developing a thermoplastic blend, the thickness of the sample is very important particularly if the thermoplastic is melted onto the surface, and no solvents are involved. If the thermoplastic is melted and blended with a more scratch resistant polymer, then the thickness of the coating can be difficult to control and this will result in a coating that is easily torn from the substrate during a routine scratch test.

"The American Society for Testing and Materials (ASTM D 907-70) defines adhesion as the 'state in which two surfaces are held together by interfacial forces which may consist of valence forces or interlocking forces or both'. These bonding forces can be the van der Waals forces, electrostatic forces and/or chemical bonding forces that are effective across the interface." Bellido-Gonzalez, Stefanopoulos and Deguilhen [29] believe that failure modes during scratch testing are the result of spalling failure at the interface (adhesive type of failure), buckling failure (sample buckles upward in front of the indenter), chipping failure within the coating itself (cohesive type of failure), conformal cracking (due to bending of the coating in front of the indenter) and tensile cracking (due to a compressive stress in front of the indenter and a tensile stress in back of the indenter). Obviously, thicker scratch resistant coatings on a substrate will be more affected by these failure mechanisms.

VII.2. Results for BLOX + LB-22 or PLC-3

Braig, Muller, Grob, Meerholz and Nuyken [30] verify that THF is an excellent solvent for non-crosslinked polymers, and it is occasionally used with some crosslinked polymers such as oxetane-functionalized homopolymers and copolymers. They inform us that their non-crosslinked precursor polymers are soluble in common organic solvents such as toluene, chloroform and THF. [30] BLOX will dissolve with some difficulty in THF suggesting that BLOX is primarily a non-crosslinked polymer with a limited amount of crosslinking present.

Our results were disappointing when using THF and the solvent method with most BLOX blends. Since this material is well known as an effect vapor barrier, the solvent and even small air molecules such as oxygen become trapped in the samples as bubbles when the solvent is being evaporated. In comparison, results for the non-solvent method at 155˚C produced good surfaces with scratch recoveries comparable to FP-1 + epoxy.

We now discuss the results for blends obtained by the non-solvent route. Plots of the residual depths versus the applied force are shown for a pure BLOX sample, 10 % LB-22 + 90 % BLOX and 10 % PLC-3 + 90 % BLOX prepared in a vacuum oven at 155˚C for 4 hours at atmospheric pressure (30.2 inches of Hg) and under vacuum (20 inches of Hg) - see Figure XVII. Plots of the corresponding penetration depths versus the applied force and the percent recovery versus applied force are also included.

10 % LB-22 + 90 % BLOX prepared at 155˚C for 4 hours at atmospheric pressure shows in Figure XVII an excellent residual depth with only 18 microns at the applied force of 14 N. Preparing this sample under the same conditions but under vacuum actually increased the residual depths over the entire range of applied forces – an undesirable effect. The residual depths for the 10 % PLC-3 + 90 % BLOX samples prepared similarly are also better than for the

pure BLOX. In this case preparing the samples under vacuum appeared to improve slightly the residual depths at applied forces above 10 N. For example, at 14 N the residual depths were 32 and 35 microns respectively for samples prepared under vacuum and at atmospheric pressure. In comparison, the pure BLOX shows a rough surface with a relatively poorer residual depth that averages significantly deeper than the 10 % PLC-3 + 90 % BLOX samples; however, some scratch recovery is possible even without the addition of PLC-3 or LB-22.

The percent recoveries versus the applied forces are shown in Figure XVIII. The plots indicate that the best results were obtained by preparing 10 % PLC-3 + 90 % BLOX at 155˚C for 4 hours under vacuum and for the 10 % LB-22 + 90 % BLOX samples prepared under the same conditions without vacuum - consistently greater than 85 % scratch recovery for each. The percent of scratch recoveries averaged about 2 % better for the PLC-3 samples and were the same, 84 %, at an applied force of 12 N. The pure BLOX sample prepared under similar conditions gave a percent recovery averaging near 70 % - a not altogether bad result but worse than in the presence of additives.

The results for penetration depths versus the applied forces are included for comparison; see Figure XIX. The results in this case are relatively similar with the exception of the 10 % PLC-3 + 90 % BLOX blend that indicated a substantially greater penetration depth when prepared under vacuum. PLC-3 is a polymer liquid crystal and can be described as a fibrous material. In addition to providing mechanical support for the BLOX matrix it is believed that the fibers may trap microscopic air pockets around the fiber. Under vacuum these microscopic air pockets are removed from around the fibers and the penetration depth increases. It is believed that the interaction of the fibrous polymer liquid crystals with the thermoplastic matrix is actually greater under vacuum with the air pockets removed since there is more fiber surface area in contact with

the matrix. This interaction appears to be beneficial by adding more resiliency to the system. Although the penetration depth increases, the residual depths are shallower at higher applied forces. The percent recovery is also at least 10 % better than for the same material prepared without vacuum at 12 N.

VII.3. FP-7 + BLOX

A fluoropolymer coded FP-7 was blended with BLOX using the solvent method previously described. FP-1, FP-2, FP-3 and FP-4 blends were also prepared in the same manner. Attempts were made to "open-up" the macromolecular chain (decrease the crosslink density) and allow the solvent to escape – this would inhibit bubble formation and permit scratch testing. Of these fluoropolymer + BLOX blends, only FP-7 gave a recoverable surface at all concentrations above 5 %. Unfortunately, a phase separation appeared at any concentration below 50 % resulting in an amber colored opaque spot that increased in size with increasing FP-7 concentration – this was the surface that was scratch tested. The indenter readily penetrated the clear areas of the samples reaching the substrate beneath. These transparent areas are believed to consist primarily of BLOX with only traces of FP-7.

Results for FP-7 + BLOX at applied forces of 2 N and 10 N are shown in Table V. In general, FP-1, FP-2 and FP-4 gave surfaces unfit for scratch testing when blended with BLOX except at the addition of 20 % fluoropolymer. A minimum of 10-15 scratches were performed for these sample; however, many of the scratches completely penetrated through to the substrate. These scratches were not included in calculating the final averages; therefore, an average of about 8 scratches / sample were used to calculate these values. In any case, the scratch test results were much better for the same fluoropolymers when blended with the ordinary commercial epoxy.

The cause of these somewhat disappointing results is attributed to the outstanding vapor barrier properties of BLOX that forms a “skin” over the surface trapping the solvent THF. This reduces the toughness of the sample and this detrimentally effects scratch recovery.

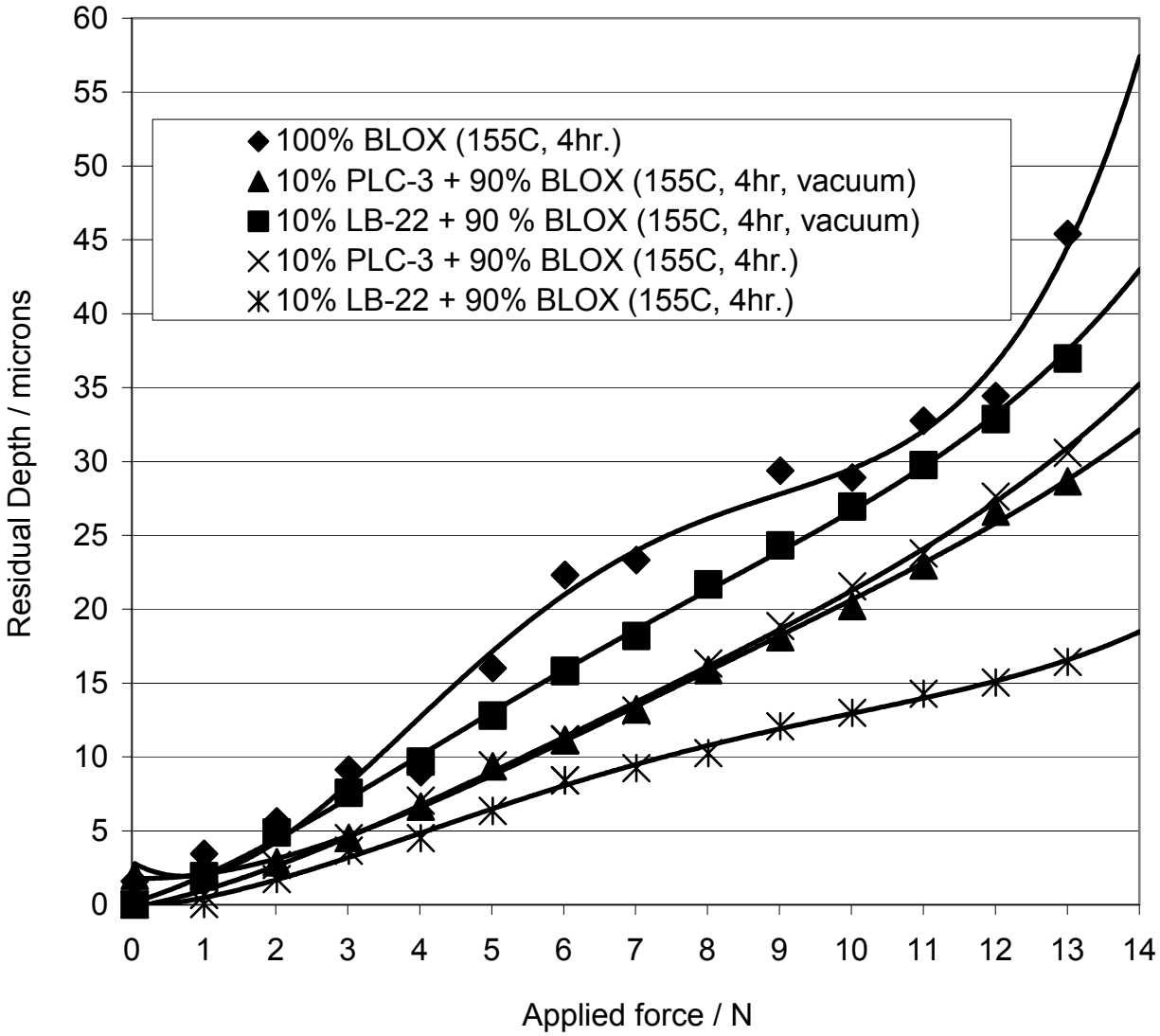

Figure XVII. Residual depth versus applied force for the BLOX blends of LB-22 or PLC-3

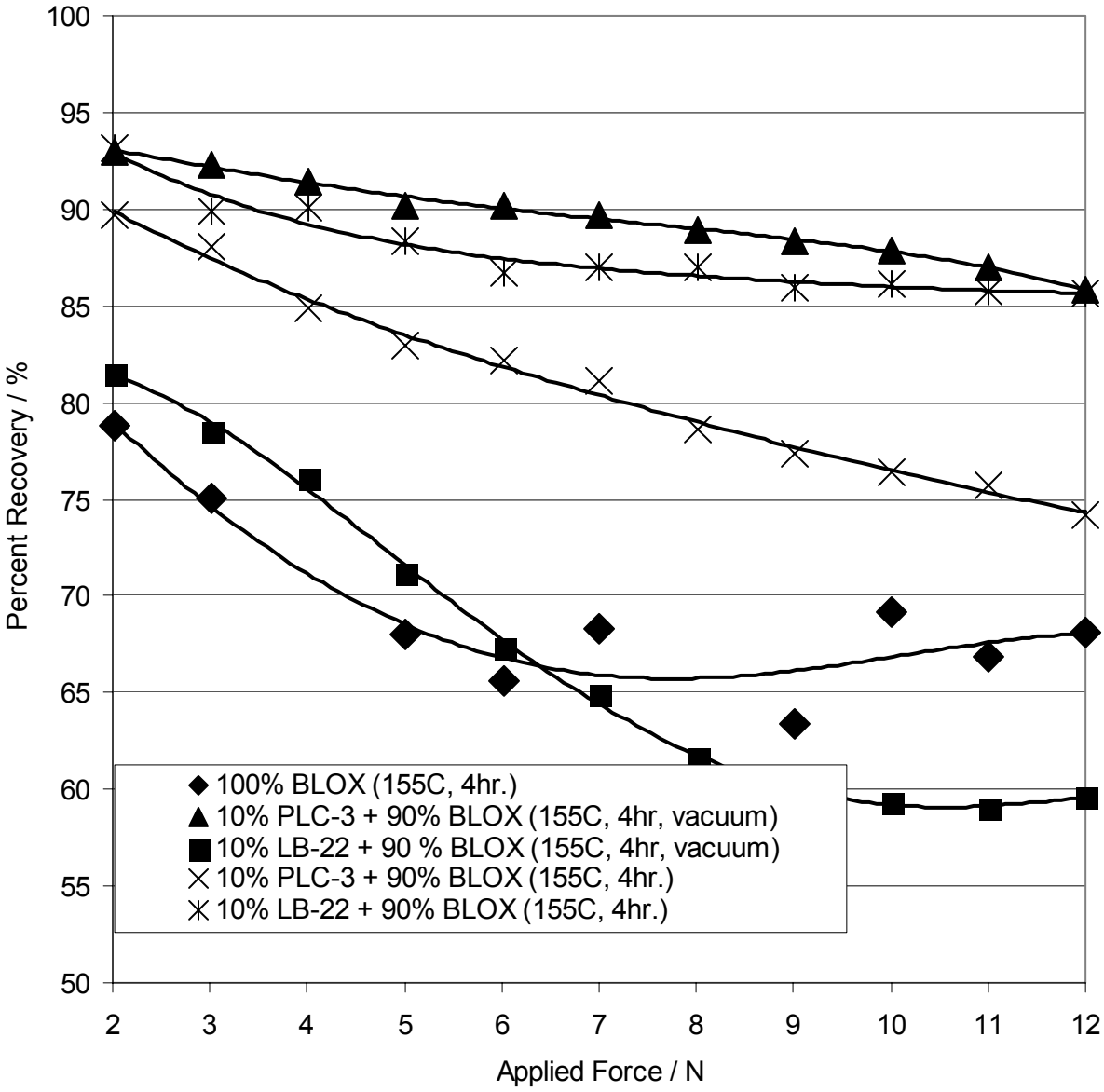

Figure XVIII. Percent recoveries of
BLOX + LB-22 or PLC-3

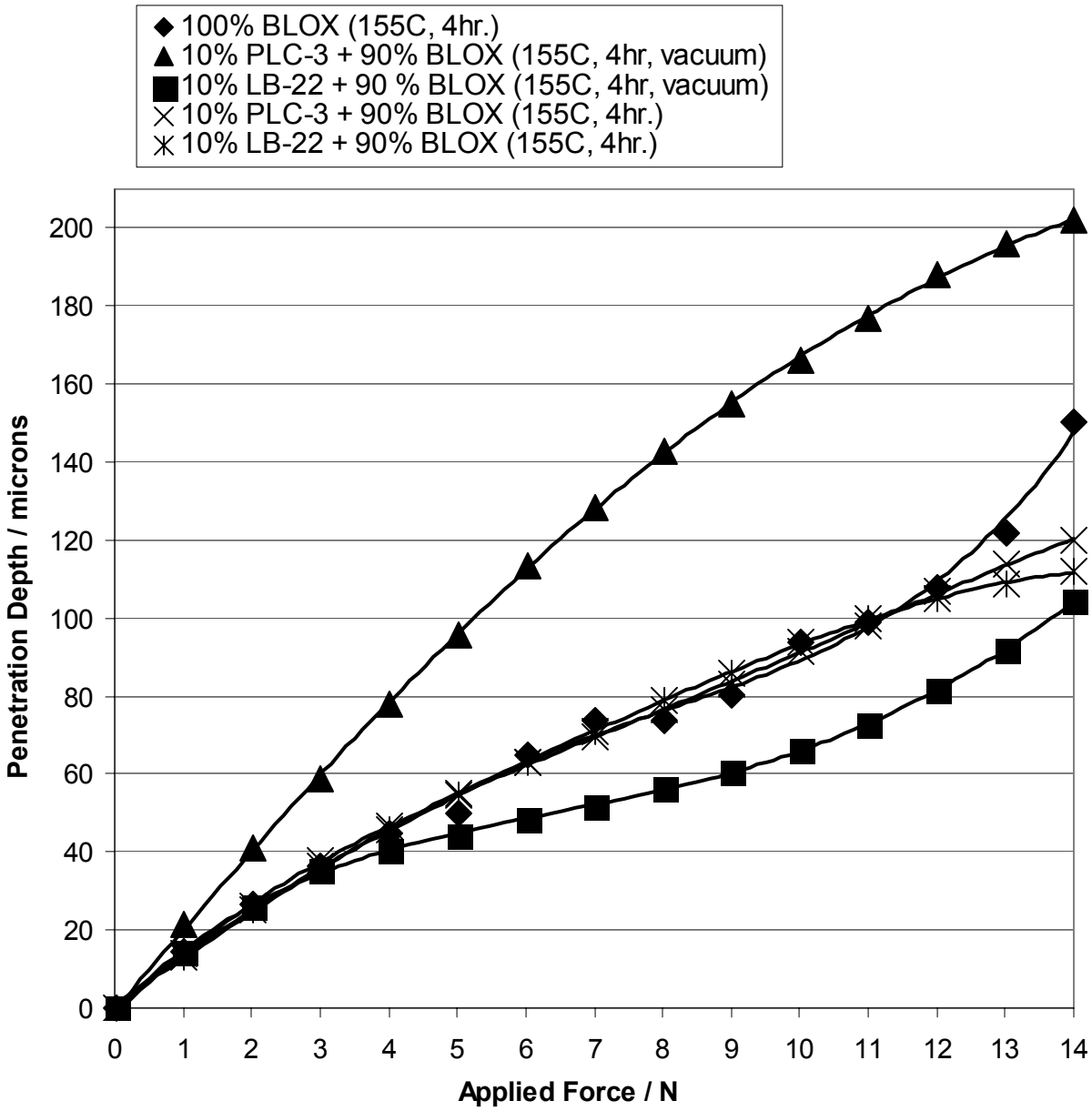

Figure XIX. Penetration depth as a function of applied force for BLOX + LB-22 or PLC-3

Table V. Fluoropolymer Addition to BLOX

(Scratch depths are in microns. Samples were cured at RT.
NA = Not Applicable – all surfaces were unfit for scratch testing.)

	2N			10N		
	PD	RD	Recovery (%)	PD	RD	Recovery (%)
0% blend	204.160	111.399	NA	NA	NA	NA
5% FP-1	349.808	203.085	NA	509.792	191.272	NA
10% FP-1	166.083	100.882	NA	NA	NA	NA
15% FP-1	151.297	97.731	NA	335.206	288.717	NA
20% FP-1	117.280	51.087	56.440	157.182	81.414	48.204
5% FP-2	270.007	157.831	NA	461.320	173.323	NA
10% FP-2	142.205	74.467	NA	307.445	204.463	NA
15% FP-2	144.469	82.542	NA	285.956	162.253	NA
20% FP-2	129.045	53.067	60.472	286.680	175.452	38.780
5% FP-3	181.951	104.812	NA	225.750	16.784	NA
10% FP-3	114.847	38.676	NA	243.347	124.728	NA
15% FP-3	98.084	63.368	NA	151.496	119.187	NA
20% FP-3	132.106	65.403	NA	359.568	195.577	NA
5% FP-4	124.315	52.998	NA	226.235	134.640	NA
10% FP-4	82.840	38.682	53.137	188.965	119.491	38.001
15% FP-4	42.223	27.611	23.985	133.279	73.801	43.562
20% FP-4	68.408	27.784	66.767	135.932	76.452	44.048
30% FP-4	107.541	44.253	58.849	186.606	105.467	43.481
5% FP-5	56.750	26.422	NA	147.679	89.701	NA
10% FP-5	99.416	52.916	NA	170.439	60.907	NA
15% FP-5	71.992	33.581	NA	131.231	51.229	NA
20% FP-5	32.505	1.582	NA	101.891	51.331	NA
5% FP-7	399.831	185.926	53.499	481.305	168.789	64.931
10% FP-7	76.311	39.101	48.760	284.165	158.585	44.192
15% FP-7	67.549	23.791	66.689	140.617	76.700	47.365
20% FP-7	69.851	32.174	53.939	222.127	120.915	45.564
30% FP-7	44.253	24.192	45.333	323.966	211.293	34.779
40% FP-7	58.844	33.654	42.808	284.949	176.617	38.018
50% FP-7	29.531	18.254	38.185	206.556	119.963	41.922
100% FP-7	30.152	4.984	83.490	88.409	43.318	49.742

CHAPTER VIII

A HYPOTHESIS FOR WHY FLUOROPOLYMERS ENHANCE SCRATCH RECOVERY

VIII.1. Non-functional and functional structural groups

The fact that the chemical structure can be correlated with some measurable property of a polymer is hardly a new idea. Several authors have proposed correlations between the chemical structure and the glass transition temperature of polymers. Their methods are usually based on the assumption that the structural groups in the repeating units provide relative additive contributions to the T_g. In the case of "ideal additivity", the contribution of a given group is independent of the nature of adjacent groups. Although this ideal case is seldom encountered in practice, additivity can often be approximated by a proper choice of structural groups. [25]

Transition temperatures are highly structure sensitive, partly due to steric effects, partly due to intra- and inter-molecular interactions. This thesis applies the same principle to the scratch resistance of polymers. Structural groups can be classified into two main types:

(a) the *non-functional structural groups* that are the building blocks of the chain. This includes methylenes (-CH_2-) and phenylenes (-C_6H_4-); in both groups the hydrogen atoms may be substituted by other elements or groups. These groups are often attacked during thermal decomposition.

(b) the *functional structural groups* originate from the condensation reactions of the functional groups in the "monomers" (such as –OH, -C=0, -NH_2, -COOH, -CF_3, etc.) These groups give the characteristic names to the polymer families, such as -oxides, -sulfides, -carbonates, -esters, -amides, -urethanes or fluoro- and often contain highly electronegative atoms. [25]

Let us consider the scratch resistance and recovery of polymers in terms of the functional groups in the monomer. The applied force of the indenter during a scratch easily breaks many of the weaker bonds (e.g., hydrogen bonds) formed by the electronegative atoms. When the indenter is removed the weaker bonds are easily reformed; however, the stronger covalent bonds that are abundant in the chain backbone are not as readily repaired. These non-functional structural groups or "building blocks" of the polymeric chain cannot be neglected though. As will be shown in Section 2, the presence of phenylenes ($-C_6H_4-$) is important in scratch recovery.

Axen, Kahlman and Hutchings [31] found significantly higher scratch recovery in *ceramics* containing an element with a high electronegativity. Scratching was performed with a standard Rockwell C diamond indenter with a spherical tip of 200 micron radius and a cone angle of 120°. The normal load was either held constant during each test at a value between 10 and 100 N or increased linearly over the scratch length of 5 mm. The test included eight silicon carbide-based engineering ceramics. Of these silicon carbides only the Si_3N_4 + SiC with the 70 volume % of Si_3N_4 revealed a predominantly plastic response to scratching throughout the load range up to 100 N, with no sharp changes in damage mechanisms. [31] It should be noted that the electronegativities of nitrogen, carbon, oxygen, silicon and fluorine are 3.0, 2.5, 3.5, 1.8 and 4.0, respectively. As the electronegativity of bonding atoms increases, the affinity for electrons increases.

Lange, Luisier, Schedin, Gunnar and Hult [32] have tried to explain why some materials demonstrate high scratch recovery and others do not. Their model is based on the crosslink density. They admit that scratch resistance is a highly desired but little understood property of coatings. "It depends on the intrinsic properties of the coating material in a way that is still largely unknown. The properties of a coating are related to the structure of the polymer

crosslinks, or crosslink density. In general, as the crosslink density is increased, the ductility of the material decreases and the hardness increases. Previous studies, using tests simulating mainly handling scratches, have shown that in some cases the scratch resistance increases with increasing crosslink density of the coating, whereas in other cases it decreases. In this work [by Lange et al., note of the present author] these tests also exhibit the same trend; an increase in scratch depth with increasing crosslinked density....a similar increase in scratch resistance with decreasing crosslink density of the coatings has been found in previous studies of polyester and urethane systems. In both these cases it was shown that the toughness (energy to break) of the coating, which increases with decreasing crosslinked density, correlated well with scratch resistance. In comparison, work on a series of epoxy coatings, in one case has shown the opposite behavior, i.e. an increase in scratch resistance for increasing crosslink density of the coating. Those results agree well with the commonly made observation that *harder materials are more scratch resistant than softer materials*. The reason why such widely different behaviors are observed remains unclear at present." [32]

Nguyen, Amgaad, Cailler, Tran and Lefrant [32] have investigated the formation of layers formed on treated surfaces of polypara*phenylene*-vinylene (PPV) substrates before and after deposition of an aluminum film. The results are discussed in relation to the adhesion property only of the metal layer on the polymer films. The scratch test measurements indicate an enhancement of the adhesive strength with Ar + O_2 and N_2 treatments; the critical loads are as much as 25 times higher as compared to the untreated samples. These results indicate to us the effect that electronegative atoms have upon the adhesive *and cohesive* forces within the sample during a scratch recovery test. [32] The electronegative atoms form molecular attractions by which the polymer chains will attempt retain the original shape of the coating. As previously

mentioned, weak bonds are present that are easily broken and repaired. These bonds are primarily responsible for the cohesive forces within the material.

Determining the atomic mass contribution from the structural groups of a molecule is not a new technique, and van Krevelen uses this technique to try and explain the properties of polymers in general. Van Krevelen writes, "If the elemental formula of the structural unit of a polymer is known, the molar mass per structural unit can be calculated directly by addition (summation) of the atomic masses. The molecular mass is the oldest Additive Function; it is additive by definition, since it is based on a fundamental law of chemistry: the law of 'Conservation of mass'. Since structural units consist of a number of characteristic structural groups, the mass structural unit can also be calculated as sum of the masses of the structural groups." [25] This thesis proposes that it is primarily the functional structural units as opposed to the building blocks of the chain that improve scratch recovery; however, both are significant. The functional structural units typically contain the highest percentage of electronegative atoms.

Friction test results for FP-4 in epoxy at various concentrations and cured at 70˚C, as previously mentioned and shown in Figure XI, indicate two areas with minimal values in the curves for both the static and dynamic friction – one at about 3 % and the other near 18 % FP-4. The 18 % minimal value for the friction results corresponds well with the 15 % minimum indicated by the scratch test results. The fact that the curves for friction and scratch testing appear very similar around 15 % is a desirable property since one would want the lowest friction and the highest scratch resistance from a material to appear at the same concentration. But why is there an additional minimal value at around 3 % FP-4 for the friction results? In order to understand what is happening in the plot of friction versus concentration of FP-4 a basic assumption must be made: a flat surface will encounter more friction that a bumpy surface. The

flat surface has more contact area with respect to the friction table. An evenly dispersed bumpy surface has less contact area with the friction table. As the contact area decreases then the friction will decrease. The friction test results can be divided into 4 regions.

Region I, below about 3 % FP-4, the curve decreases. This is due to the presence of almost entirely epoxy at the surface, a primarily flat surface that is steadily increasing with FP-4 at the surface. The FP-4 will initially form small rounded islands at the surface and this will decrease the contact area and decrease friction.

In region II, as the concentration of FP-4 is increased from around 3 % to 10 % FP-4, the islands begin to grow larger in diameter and the epoxy becomes less prominent at the surface. This results in an increase in the contact area and the friction begins to increase again.

In region III, about 10 % to 18 % FP-4, the epoxy begins to leave "holes" as the FP-4 continues to dominate the surface – the islands grow taller relative to the epoxy. This again causes a decrease in the contact area and a corresponding decrease in friction since the "holes" left by the receding epoxy now decreases the contact area.

In region IV, above 18 % FP-4, the FP-4 begins to fill the "holes" left by the epoxy. This results in an increase in contact area again as in region I. However, a phase inversion has taken place and FP-4 dominates the surface whereas in region I, the epoxy dominated the surface. The result is essentially the same in either case – a flat surface will cause more friction than a surface with islands. Suggestions for future research include using SEM to verify this proposed effect.

During the scratch testing of FP-4 + epoxy samples it was observed that these samples were rather difficult to mount to the scratch test table, the bottom surfaces of the samples were too "slippery" – a phenomenon not observed with FP-1, FP-2 or FP-3. The friction results from the bottom surfaces of the samples are also indicated for comparison with the top surfaces. The

graphs follow the same pattern in each case; however, the friction is higher for the bottom of the sample due to a higher concentration of FP-4 remaining at the top surface. Island formation will have more of an effect on the top surface. Although it appears that FP-4 is preferentially migrating to the top surface, some FP-4 is going to the bottom surface due to the density effects discussed in Section 4 of Chapter VI.

VIII.2. Hypothesis: "More is not better!"

For the series of successful polymers FP-1 through FP-4, there was also a series of unsuccessful fluoropolymers – FP-5 and FP-6. Unsuccessful fluoropolymers are obviously much easier to create than successful ones. A fluoropolymer is unsuccessful for various reasons. Extensive phase separation on the surface of blends in which the samples have large areas of surface not containing any FP is one of the most common difficulties in using FPs to enhance scratch resistance. This results in some areas of the surface demonstrating high scratch recovery while the scratch indenter may completely tear through the surface of unprotected areas.

Another problem frequently encountered in using fluoropolymers for the task at hand is that the final blend of FP + epoxy may not contain the optimal concentration of fluorines, carbonyls or phenylenes. More is not better! By increasing the amount of fluorines in a molecule one does not necessarily increase the amount of scratch depth recovery. Table VI illustrates this point. It appears that the optimum range for scratch depth recovery occurs when the pure fluoropolymer contains less than 14 % fluorine atoms. Taking half of this amount or 7 % appears to be not quite enough to give optimum scratch recovery - as in the case of FP-2.

In general, optimum scratch recovery occurs when there is less than 10 % of fluoropolymer in the epoxy blend. However, as Figures XII through XIV suggest, the optimum concentration may

vary above or below 10 % depending on the chemical structure of the fluoropolymer, namely the weight percent of fluorine in the pure fluoropolymer. Each monomer of FP-1 or FP-3 has 12 fluorines while each monomer of FP-2 or FP-4 has 6 fluorines. Indeed, the minimum in the residual depth versus percent fluoropolymer is shown to lie around 6 % for FP-1 and FP-3 while the minimum for FP-2 and FP-4 is approximately double that, namely 14-15 %.

Table VI also indicates that besides the weight percent of electronegative atoms, the proper weight percent of carbonyls and phenylenes is important in scratch depth recovery. Teflon, which has relatively poor scratch recovery, has an electronegative composition of 76.0 weight percent (66.7 atomic percentage) entirely of fluorines. Teflon also has 0 weight percent of carbonyls and phenylenes. Apparently, not only does an appropriate concentration of electronegative atoms increase scratch recovery but also the presence and appropriate concentrations of carbonyls and phenylenes play a role in improving scratch depth and recovery.

Theoretically, could one substitute other electronegative atoms such as oxygens in place of the fluorines and still achieve significant increases in scratch depth recovery? There is very significant evidence that this is true. Column I in Table VI indicates that the optimum atomic percentage of electronegative atoms is around 9 - 14 % - these are electronegative atoms not located directly between a carbonyl and a phenylene or some combination of the two groups that would cause steric hindrance. An oxygen located directly between a phenylene and a carbonyl is not counted in the atomic percentage of free electronegative atoms. However, when it is not sterically hindered then in theory it will be freer to participate in bonding (e.g., hydrogen bonding) with other side chains within the epoxy. A carbonyl oxygen atom does not appear in Column I under atomic percentage of free electronegative atoms, it is counted as part of the carbonyl group under Column III.

It is somewhat misleading to write the carbonyl as a covalent C=O double bond. The difference between the electronegativities of carbon and oxygen is great enough to make the C=O bond slightly polar. As a result, the carbonyl group is best described as a hybrid of the following resonance structures shown in Scheme 1 below.

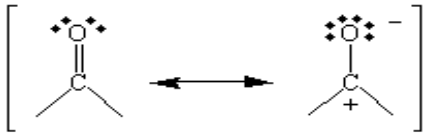

This creates a potential for the carbonyls (ketones) within a polymer chain to form secondary alcohols through a reduction reaction and for the secondary alcohols to form carbonyls (ketones) by an oxidation reaction. Therefore, for these reasons, secondary alcohol groups within a polymer are counted along with the carbonyls in Column III. It should be noted that carbonyls readily form weak hydrogen bonds.

Column IV surprisingly indicates that the most abundant component in these high scratch resistant systems are the phenylenes, the so-called non-functional structural groups of the chain backbone - not the electronegative atoms. The reason for this is not entirely understood. The optimum range for phenylenes in a pure fluoropolymer is 38 – 54 %.

Among the pure fluoropolymers FP-1 through FP-7 only FP-1, FP-4 and FP-7 have values that lie within the optimum range for each column. Table V, as previously discussed, suggests that the scratch recovery is improved by developing fluoropolymer blends that "open-up" the long macromolecular chains and allow the solvent to escape. Therefore, this is an additional factor to consider with an effective vapor barrier material such as BLOX. It should be noted that of the fluoropolymers investigated the monomer of FP-7 was the smallest molecule.

Table VI: Comparison of Pure Fluoropolymers

	I	II	III	IV
	Free electronegative atoms			
	atomic %	weight %	wt % -C=O[¶]	wt % Phenylenes
FP-1	**14.3**	**27.0**	**6.6**	**54.1**
FP-2	7.2	15.5	7.6	61.9
FP-3	18.8	32.9	8.1	44.0
FP-4	**9.4**	**16.5**	**9.6**	**52.1**
FP-5	4.5	11.4	11.6	45.5
FP-7	**14.3**	**28.5**	**14.0**	**38.0**
teflon	66.7	76.0	0	0
epoxy	5.6	12.5	6.4	52.1
Optimum range:	**9-14**	**16-28**	**6-14**	**38-54**

[¶] Secondary alcohols are counted under Column III because of their potential to undergo oxidaton to form carbonyls (ketones) and visa versa. Suggestions for future research include investigating the scratch resistance for novel and existing polymers containing structural groups with sulfur-oxygen double bonds since each sulfur atom may form two oxygen double bonds as indicated in Table III. This might vary the optimum range for Column III.

CHAPTER IX

HYPOTHESIS FOR WHY BLOX EXHIBITS GOOD SCRATCH RECOVERY: OXYGEN AND NITROGEN ELECTRONEGATIVITY

Budinski [34] writes that attempts were made to explain scratch recovery on the basis of the hardness of various plastics. "Unfortunately there is no single plastic hardness scale that is suitable for the wide range of plastics/elastomers included in this study. It was thought that the resilience of the plastics may play some role in resisting indentation and scratching by hard particles....however, these rebound hardnesses did not show an apparent correlation with the abrasion volume losses." Budinski also adds that "the wear test results did not correlate with any of these scratch test results (either)." [34]

Jia, Pang and Huang [35] report successfully making copolymers in THF. "Copolymerization of maleimide (MI) and ethyl α-(hydroxymethyl)acrylate (EHMA) was performed at 60˚C with α,α'-azobisisobutyronitrile (AIBN) as the initiator in THF. TGA diagrams suggested the crosslinking reaction of the copolymer on heating." However, their work does not report any scratch test data or any information about the hardness of the resulting polymers produced in THF solvent. [35] One recalls that the BLOX blends produced at LAPOM have rather poor scratch recovery as compared to those without using THF as a solvent.

Ochi, Onlshl and Ueda [36] also used THF as the solvent to develop a useful copolymer. However, in this case the THF became part of the chain through copolymerization and was not simply just a solvent. "Naphthalene-type epoxy resin was cured with u.v. irradiation in the presence of tetrahydrofuran (THF) using sulphonium salt as a curing catalyst. In this process, the epoxy resin was copolymerized with the THF. Thus evaporation of THF was suppressed substantially. The suppression of solvent evaporation decreased shrinkage of the coatings in the

curing process.... Fracture energy of these cured films increased with the amount of THF added, and had a maximum value when 10 wt % of THF was added. This shows that the toughness of the cured resins increases with the introduction of the flexible chains which were formed by the ring-opening reaction of THF." [36] Ochi, Onlshl and Ueda thus confirm our findings that THF may increase toughness by "opening-up" the macromolecules; however, a higher concentration of THF remaining in a copolymer will decrease the toughness of the scratch surface. We believe (in this case) that this effect is also due to a decrease in crosslink density – see Table V. As the crosslink density is decreased, the matrix becomes more soft and pliable.

Rapoport, Lapsker and Levin [37] also report similar findings to LAPOM regarding the increase in the relative wear resistance of a material by introducing nitrogen. "Nitrogen ion implantation has been found to increase the wear resistance of glassy carbons by a factor at least 100 over that of the unimplanted material." [37]

Pure BLOX has a fairly good scratch recovery as indicated in Chapter VII. There are no fluorines present in BLOX; however, there are also a significant number of oxygens. Phenylenes, classified as non-functional structural groups by van Krevelen, compose a large portion of the chain backbone in BLOX. This concept will be developed further in Chapter XI.

CHAPTER X

A HYPOTHESIS FOR WHY PLC-3 IMPROVES SCRATCH RECOVERY OF THERMOPLASTICS

Beaumont, Farris and Sun [38] conducted scratch tests using a friction table with an applied load up to 40 N on fibrous containing polymers. "The fibers were cut at all orientations. The slip-stick interaction between the indenter and the surface (occurs when) the indenter gets caught by some fibers bridging the furrow. As the indenter continues to slide along the furrow, the tangential load builds up until the stress is high enough to break the fibers, after which, the indenter jumps slightly, and the instruments record a drop in the coefficient of friction. To extrapolate these results for the case of multiple indenter (passes)....fiber orientation would still not have much effect on the energy needed to abrade the surface, and the surface, while becoming damaged, would not wear as fast as a monolithic material due to the presence of the fibrous wear particles assuming normal applied loads less than 40 N per scratch." [38]

Mechanical reinforcement, as Beaumont and coworkers suggest, plays an important role in improving scratch recovery of many fiber-containing polymers. Scratch test results of PLC-3 + BLOX suggest that the high scratch recovery of this polymer liquid crystal in the BLOX matrix increases primarily due to the mechanical reinforcement by the fibrous PLC. The randomly oriented fibers are clearly seen with the unaided eye, not only by optical microscopy.

CHAPTER XI

A HYPOTHESIS FOR WHY LB-22 IMPROVES SCRATCH RECOVERY OF THERMOPLASTICS

Although PLC-3 + BLOX is easily explained by the reinforcement properties of the polymer liquid crystal fiber structure in the BLOX matrix, the combination of LB-22 + BLOX is not so easily explained. The functional structural components in LB-22 include oxygens found in carbonyls and as a part of 6-membered ring systems that are located both on side chains and as part of the main chain backbone. A concentration of 13 % plasticizer is added to LB-22, and this supplies the phenylenes ($-C_6H_4-$) as well as more carbonyls. The final composition of LB-22 includes ample non-sterically hindered oxygens, carbonyls and phenylenes. In LB-22 without additives there are no phenylenes.

It is worth noting that one can theoretically engineer the side chains in LB-22 so that the concentration of oxygens becomes nearly 1/2 of the total in the macromolecule. This is above the optimum range calculated for the pure fluoropolymers already given in Column II of Table VI that lists the optimum weight percent of electronegative atoms at 16-28 % based on the pure fluoropolymers. Since most of the oxygens in LB-22 are sterically hindered by the presence of neighboring carbonyls and non-aromatic rings, the concentration of free electronegative atoms in LB-22 is actually quite lower.

It is the combination of LB-22 with BLOX that leads to excellent scratch resistant properties. BLOX itself contains an abundance of phenylenes (even if they were not present in the plasticizer) and free electronegative oxygens and nitrogens; however, it normally does not contain any carbonyls unless one assumes that the secondary alcohols are eventually converted to carbonyls. In any case, LB-22 (+ plasticizer) supplies functional carbonyl groups.

The mechanism by which LB-22 (+ plasticizer) + BLOX improves scratch recovery appears to be very similar to that of FP-1 + epoxy except that there are no fluorines present. Oxygens and nitrogens supply the electronegative atoms. The optimum ratio of free electronegative atoms, carbonyls and phenylenes for LB-22 (+ plasticizer) + BLOX, as in the case of FP-1 + commercial epoxy, make these excellent scratch recovery materials.

The percent of scratch recovery for the blend of 10 % LB-22 + 90 % BLOX is actually higher than for the pure components, see Figure XX. The 100 % BLOX contains no additives, the pellets are pulverized then melted and no additional plasticizers are added to LB-22. In most cases the dependence on the applied force is only weak. At 12 N, the percent recovery of the LB-22 blend is at least 17 % higher than the pure BLOX and 10 % higher than LB-22 alone.

It is interesting to note that doubling the concentration of LB-22 in BLOX to 20 % in effect *decreases* the percent recovery by an average of 14 % compared to the 10 % LB-22 blend; for brevity this graph is not shown. This agrees with the hypothesis that “more is not better”. For comparison, the best percent recoveries defined during this stage of work are summarized in Figure XXI.

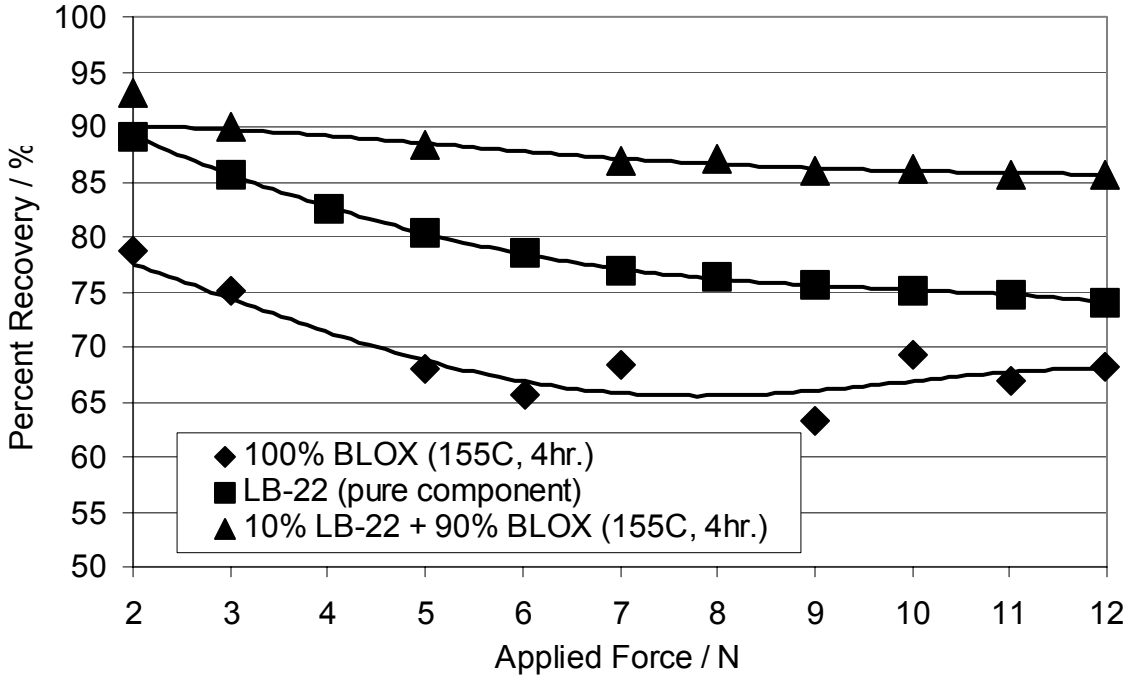

Figure XX. Percent recoveries of 10 % LB-22 + 90 % BLOX compared to the pure components

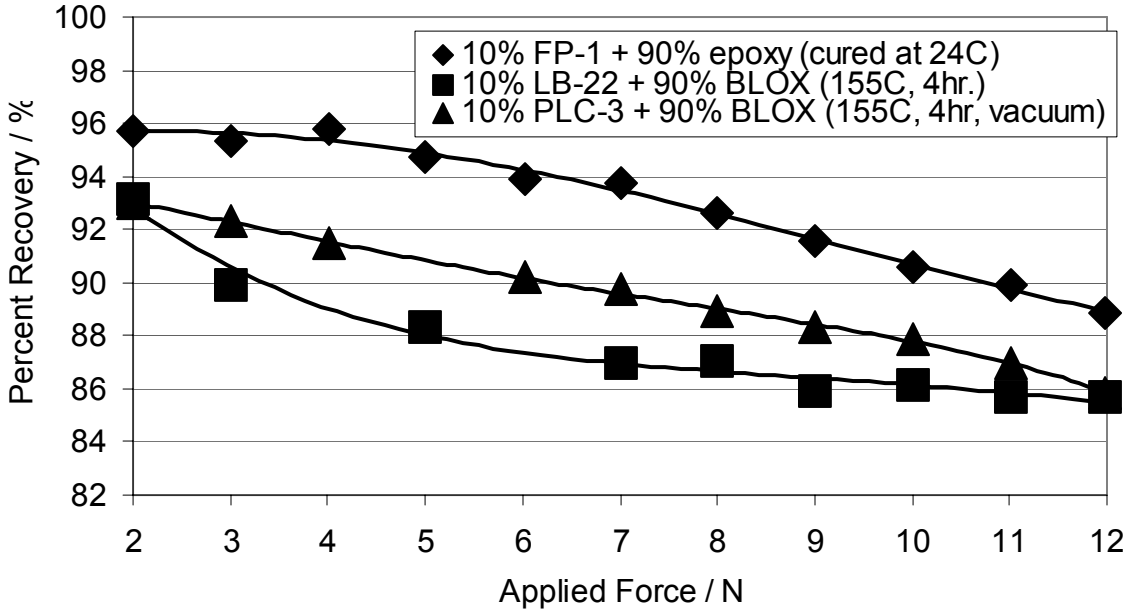

Figure XXI. The best percent recoveries

CHAPTER XII

CONCLUSIONS AND SUMMARY OF MODEL FOR OPTIMUM SCRATCH RECOVERY

Consider the results of Bhushan and Lowry [39] for ceramics. The wear of various head materials was run against a highly abrasive tape sample, CrO_2, for evaluation of their wear characteristics. Single phase ceramic materials Mn-Zn ferrite, $CaTiO_3$, SiC, two phase Al_2O_3 + TiC and an amorphous glass were all tested against a magnetic tape in an accelerated wear test. The most wear resistant material was the two phase Al_2O_3 + TiC. This demonstrates that two-phase polymer systems can provide better scratch resistance than one-phase ones. [39]

Tan, Prabhakaran and Talke [40] argue that wear is a function of several parameters and no single measurement such as hardness should be used to predict it. "Archard's wear law predicts that hard materials wear less than soft materials. Since hardness is an important mechanical property of magnetic head materials, hardness measurements are widely used to characterize the tribological performance of potential head materials. However, the wear mechanism of the magnetic head/tape interface is not only a function of the hardness of the head material but also a function of tape drive design parameters, tape tension and tape velocity. Thus, it is difficult to fully characterize the wear behavior of the head/tape interface using a simple equation." [40] The purpose of this thesis is to thoroughly investigate one of the most important wear parameters – scratch recovery. Harsha and Tewari [41] suggest that a more complete determination of wear would include measuring the loss in weight of the polymer (after abrasive wear studies) and then converting this information to wear volume using density data. Unfortunately, this does not take

into account the build-up of material in front of the indenter or alongside the scratch that may occur during scratch testing – one may also consider this as wear.

It has been shown in this work that several fluoropolymers when blended are effective in scratch recovery. FP-1 and FP-4 both give excellent scratch recovery. FP-1 is better – consistently demonstrating a percent recovery above 90 % when cured at 24˚C. Oxygens can often replace fluorines in designing new materials; however, the effectiveness of scratch recovery is also highly dependent upon the degree of electronegativity – a sample containing atoms with higher electronegativity would be expected to have a higher scratch recovery. When one is looking at a chemical bond to predict whether it is polar (and the direction of polarity) one must compare the electronegativities of the atoms in the bond. The atom with the higher electronegativity will have the negative end of the polar bond, and the difference in electronegativities will give a rough approximation of the extent of the polarity. A greater polarity will increase the probability of forming a weak bond such as a hydrogen bond. Weak bonds are easily broken and reformed during a scratch test. A table of electronegativities for the main group elements is provided at the end of this chapter.

Scratch recovery is a complex phenomenon related to factors such as the weight percent of the sterically unhindered electronegative atoms and the presence of carbonyls and phenylenes in the macromolecule. More is not necessarily better! In general, increasing the weight percent (concentration) of fluoropolymer in an ordinary commercial epoxy above 10 % will not improve scratch recovery. On the molecular level, there is no indication that increasing the weight percent of fluorines in a pure fluoropolymer above 16 – 28 % will improve scratch recovery.

BLOX resins offer a unique set of properties, including good adhesion to a variety of substrates, high gas barrier performance, good mechanical strength and toughness. [42,43] The

present work has shown that the excellent scratch resistance of pure BLOX is further enhanced with only a 10 % addition of either LB-22 or PLC-3. These materials represent possible cheaper alternatives for high scratch recovery materials than fluoropolymer systems.

Historically, hardness and crosslink density have been used to explain the scratch resistance of a material. The aim of this work is to give the reader a more accurate picture of the mechanisms involved in polymer systems that recover.

Table VII: Electronegativities for the Main Group Elements

H = 2.1	x	x	x	x	x	x
Li = 1.0	**Be =** 1.5	**B =** 2.0	**C =** 2.5	**N =** 3.0	**O =** 3.5	**F =** 4.0
Na = 0.9	**Mg =** 1.2	**Al =** 1.5	**Si =** 1.8	**P =** 2.1	**S =** 2.5	**Cl =** 3.0
K = 0.8	**Ca =** 1.0	**Ga =** 1.6	**Ge =** 1.8	**As =** 2.0	**Se =** 2.4	**Br =** 2.8
Rb = 0.8	**Sr =** 1.0	**In =** 1.7	**Sn =** 1.8	**Sb =** 1.9	**Te =** 2.1	**I =** 2.5
Cs = 0.7	**Ba =** 0.9	**Tl =** 1.8	**Pb =** 1.9	**Bi =** 1.9	**Po =** 2.0	**At =** 2.2

REFERENCES

1. Heavens OS (1950) J. Phys. & Radium 11: 355

2. Benjamin P, Weaver C (1960) Proc. Royal Soc. A 254: 163

3. Steinmann PA, Hintermann HE (1985) J. Vac. Sci. Technol. A 3: 2394

4. Kody RS, Martin DC (1996) Polymer Eng. & Sci. 36: 298

5. Williams JA (1996) Tribology Internat. 29: 675

6. Bull SJ (1999) Wear 233-235: 412

7. Ahila S, Reynders B, and Grabke HJ (1996) Corrosion Science 38: 1991

8. ASTM Standard D – 1894 – 90

9. Brostow W (1985) Science of Materials. Robert E. Krieger Publishing Company. Malabar, Florida

10. Spuzic S, Strafford KN, Subramanian C, Green L (1995) Wear 184: 83

11. Bennett S, Matthews A (1995) Surface & Coatings Techn. 74-75: 869

12. Benayoun S, Hantzpergue JJ, Bouteville A (2001) Thin Solid Films 389: 187

13. Consiglio R, Randall NX, Bellaton B, von Stebut J (1998) Thin Solid Films 332: 151

14. Hedenqvist P, Hogmark S (1997) Tribology Internat. 30: 507

15. Jardret V, Zahouani H, Loubet JL, Mathia TG (1998) Wear 218: 8

16. Malzbender J, de With G (2001) Thin Solid Films 386: 68

17. Randall NX, Favaro G, Frankel CH (2001) Surface & Coatings Techn. 137: 146

18. Brostow W, Cassidy PE, Hagg HE, Jaklewicz M, Montemartini PE (2001) Polymer 42: in press

19. Brostow W, Bujard B, Cassidy PE, Hagg HE, Montemartini PE (2002) Mater. Res. Innovat. 6: to be published

20. Roy, R (1990) A Primer on the Taguchi Method. Van Nostrand Reinhold, New York

21. Fouad A, Johannesson T (1996) Surface & Coatings Techn. 78: 87

22. Liew T, Wu SW, Chow SK, Lim CT (2000) Tribology Internat. 33: 611

23. Gedde UW (1999) Polymer Physics, Kluwer Academic Publishers, Amsterdam

24. Hill LW (1992) Coatings Techn. 64: 29

25. van Krevelen DW (1990) Properties of Polymers, 3rd ed. Elsevier Science Publishers, Amsterdam

26. Fossey SA, Tripathy S (1999) Internat. Biol. Macromolecules 24: 119

27. Carlsson P, Bexell Ulf, Olsson M (2001) Wear 247: 88

28. Ashrafizadeh F (2000) Surface & Coatings Techn. 130: 186

29. Bellido-Gonzalez V, Stefanopoulos N, Deguilhen F (1995) Surface & Coatings Techn. 74-75: 884

30. Braig T, Muller DC, Grob M, Meerholz K, Nuyken O (2000) Macromol. Rapid Commun. 21: 583

31. Axen N, Kahlman L, Hutchings IM (1997) Tribology Internat. 30: 467

32. Lange J, Luisier A, Schedin E, Gunnar E, Hult A (1999) Mater. Processing Techn. 86: 300

33. Nguyen TP, Amgaad K, Cailler M, Tran VH, Lefrant S (1995) Synthetic Metals 69: 495

34. Budinski KG (1997) Wear 203-204: 302

35. Jia X, Pang Y, Huang J (1998) J. Polymer Sci. Chem. 36: 1291

36. Ochi M, Onlshl K, Ueda S (1992) Polymer 33: 4550

37. Rapoport L, Lapsker I, Levin L (1998) Surface & Coatings Techn. 105: 117

38. Beaumont M, Farris TN, Sun CT (1997) Composites A 28A: 683

39. Bhushan B, Lowry JA (1995) Wear 190: 1

40. Tan S, Prabhakaran V, Talke FE (2000) Tribology Internat. 33: 673

41. Harsha AP, Tewari US (2002) Polymer Testing: in press

42. Glass T, Pham H, Winkler M (2000) Proc. Ann. Tech. Conf. Soc. Plast. Engrs. 46: 1813

43. White JE, Silvis HC, Winkler MS, Glass TW, Kirkpatrick DE (2000) Adv. Mater. 12: 1791